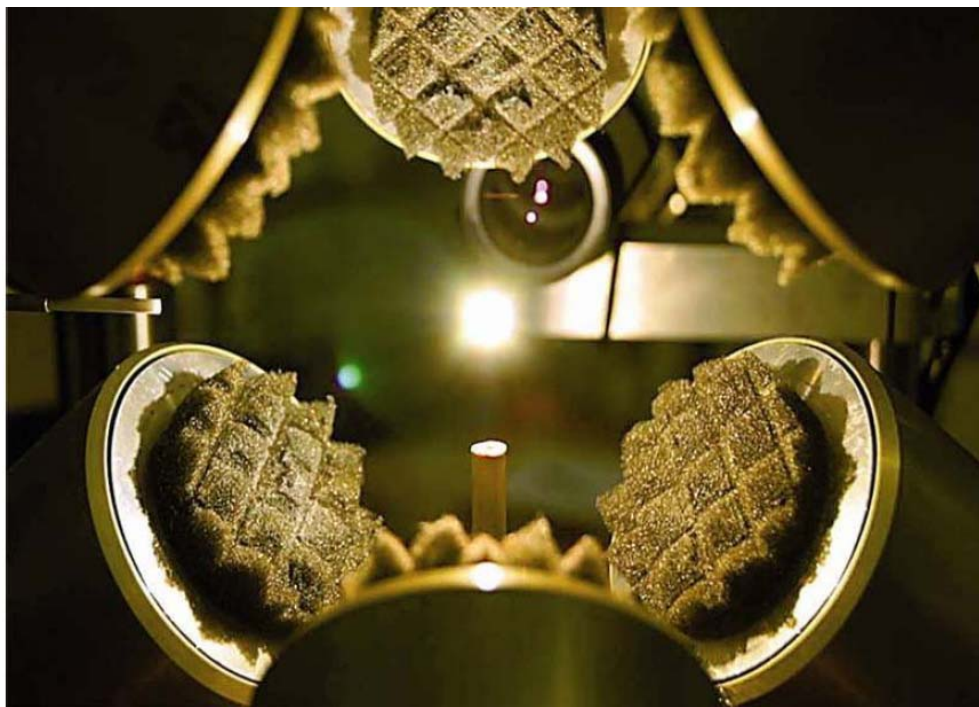


AERO-ACOUSTIC LEVITATOR

MODEL AAL 3.1

OPERATOR'S MANUAL 3.3



**Physical Property Measurements, Inc.
825 Chicago Avenue
Evanston, Illinois USA 60202
Telephone 847 864 8509 Fax 847 864 9114**

TABLE OF CONTENTS

1.	Introduction.....	1
2.	System Frame.....	3
2.1	Par Frame Structure	5
2.2	Newport Breadboard AAL Mounting Surface.....	5
3.	Levitator Structure and Components	6
3.1	Levitator Frame.....	6
3.2	Centering Device – “Chessman”	6
3.3	Acoustic Transducers.....	6
3.4	Position Sensing System	8
3.5	Gas Jet.....	9
3.6	Specimen Injector	10
4.	Electronic Components.....	11
4.1	Acoustic Amplifiers.....	11
4.2	Acoustic Controller.....	11
4.3	Sensor Detector Electronics.....	12
4.4	Power Panel	14
4.5	MKS Gas Flow Controller	15
4.6	IOLAN Device Server	15
4.7	Electrical Supply Lines.....	15
4.8	Synrad CO ₂ Laser Electronics	15
5.	Instruments.....	16
5.1	Video Cameras.....	16
5.2	Video Recorder - Monitor.....	16
5.3	Vision Research Fast Camera and Infinity Lens.....	17
5.4	Exactus Pyrometer	18
5.5	Gas Heater Control	18
5.6	Laser Hearth Melter	19
5.7	CO ₂ Lasers	20
5.8	Graphical User Interface, GUI.....	21
5.8.1	AAL Console Screen	21
5.8.2	AAL Sensors Screen.....	21
5.8.3	AAL Laser Power Screen	23
5.8.4	Exactus Pyrometer Screen	23
5.8.5	AAL Scope Screen.....	24
5.9	Computer and Software	25
5.9.1	Sensor Sensitivity Scans	26
5.9.2	Transducer Electrical Characteristics	27
5.9.3	Resonant Frequency Calibration.....	29
5.9.4	Exactus Pyrometer Data.....	31
5.9.5	Sensor Data Acquisition	32
5.9.6	AAL Operating Parameters.....	32
5.9.7	Entry of Calibration Constants.....	34
5.9.8	Programming the Acoustic and Sensor Circuits.....	35

5.9.9	Laser Power Log.....	35
5.9.10	Software Extensions.....	36
6.	Utility Requirements.....	36
6.1	CO ₂ Laser Cooling.....	36
6.2	Electrical Power.....	36
6.3	Levitation Gas.....	37
7.	Levitation and Materials Processing.....	37
7.1.	Start-up.....	37
7.2	Controls.....	39
7.3	Initial Levitation.....	40
7.4	Heating and Melting.....	41
7.5	Acoustic Modulation.....	42
8.	Transducer Calibration.....	43
9.	Transducer Algorithms.....	45
9.1	Operator- and Computer-controlled Parameters.....	45
9.2	Computer-Acquired Parameters.....	46
9.3	Calculated Parameters.....	46
9.4	Voltage, Current, I-V Phase Difference, Amplifier Power.....	46
9.5	Acoustic Frequency Control.....	47
9.6	Voltage Control to Maintain a Given Value for the SPL.....	48
10.	Transducer alignment.....	49
11.	Acoustics.....	52
11.1	Reflected Sound Waves.....	52
11.2	Sample Oscillation.....	53
11.3	Spin Control.....	55
11.4	Effect of Sample Heating.....	55
12.	Gas jet.....	56
13.	Position Sensing Operations.....	58
13.1	Feedback Control for Damping Oscillation of Levitated Samples.....	59

LIST OF FIGURES

Figure 1	Aero-Acoustic Levitation System.....	2
Figure 2	AAL System showing the frame, CO ₂ lasers, levitator, electronics and instruments.	3
Figure 3	Plan and elevation views of the AAL system with dimensions in mm and inches.	4
Figure 4	Levitator structure and components.....	6
Figure 5	Acoustic transducer.....	7
Figure 6	Position sensing system, diode laser source (top) and detector assembly (bottom).....	8
Figure 7	Gas jet assembly.....	9
Figure 8	Photograph of the gas jet assembly.....	9
Figure 9	Interior of the acoustic controller.....	12
Figure 10	Acoustic controller circuits: communication top, transducer control bottom.....	13
Figure 11	Sensor electronics: analog left, digital right.....	14
Figure 12	AAL power panel.....	15
Figure 13	Video camera, lens, neutral density filter.....	16
Figure 14	Video monitor and laser cut-off switch.....	16

Figure 15	Vision Research camera and Infinity long distance microscope lens.	17
Figure 16	Exactus pyrometer and positioning device.	18
Figure 17	Laser hearth melter for sample preparation.	19
Figure 18	Hearth-melted oxides.	19
Figure 19	Microstructure of $ZrSiO_4$ formed in the laser hearth melter.	20
Figure 20	CO_2 laser beam delivery assembly.	20
Figure 21	AAL console screen.	22
Figure 22	AAL sensor screen.	22
Figure 23	Laser power screen.	24
Figure 24	Exactus pyrometer screen.	24
Figure 25	AAL scope screen.	25
Figure 26	Acoustic transducer calibration facility.	44
Figure 27	SPL and amp power vs frequency.	44
Figure 28	Resonant frequency (FR) minus frequency (F) vs I-V phase difference.	44
Figure 29	SPL vs amplifier power delivered to the transducer motor.	45
Figure 30	Resonant frequency tracking for a typical experiment, SPL = 0.9.	48
Figure 31	Top view of levitator.	50
Figure 32	Video camera views of levitated styrofoam during acoustic alignment.	51
Figure 33	Transducer calibration for off-resonant levitation.	52
Figure 34	Resonant frequency and spring constant for harmonic vibration of acoustically-levitated Styrofoam.	54
Figure 35	Maximum density for acoustic levitation vs SPL value, estimated from the results of oscillation frequency measurements on a Styrofoam sample.	54
Figure 36	Levitation in an inclined gas jet.	56
Figure 37	Density of 2.5 mm specimens levitated in nitrogen.	57
Figure 38	Reynolds number, Re , of a nitrogen jet at 300, 536, and 800K.	57
Figure 39	Estimated density of 3 mm specimens levitated in argon and nitrogen jets.	58
Figure 40	Sensor output vs position of a levitated sample.	59

LIST OF TABLES

Table 1	TSLOTS frame specifications.	5
Table 2	Newport table specifications.	5
Table 3	Levitator components.	6
Table 4	Exactus pyrometer specifications,	18
Table 5	Calibration of transducer electrical characteristics*	29
Table 6	Resonant frequency calibration data.	30
Table 7	AAL operating parameters.	33
Table 8	Calibration constants, March 21, 2011.	49

1. Introduction

The Aero-Acoustic Levitator (AAL) instrument enables containerless processing and property measurements on solid and liquid materials at very high temperatures. It provides an ideal environment in the study of molten materials by eliminating containers that would react with and contaminate materials. Property measurements by optical, mechanical, video, and other methods are enabled by direct open access to levitated materials.

The AAL applies CO₂ laser beam heating to heat and melt levitated 0.25-0.35 cm diameter samples at temperatures up to and above 3000°C. Process gases may include air, argon, oxygen, nitrogen and others.

Levitation occurs by the aerodynamic force from an upward flowing gas jet. Acoustic forces generated by high intensity standing waves stabilize the levitation. The acoustic forces are themselves stabilized by the gas flow, which yields a stable thermal boundary layer around heated samples. Active feedback control of the acoustic forces, based on specimen position measurements, permits rapid heating, cooling and melting processes. Stable continuous operation with solid and liquid samples is possible for many hours.

A picture of the AAL system and a close-up of the levitator are given in Figures 1 and 2. The components of the system are described in parts 2-5 of the manual. Parts 6-10 describe operation calibration, alignment of the instrument. Parts 11-13 discuss the acoustic, gas jet, and position sensing phenomena and operations.



Figure 1 Aero-Acoustic Levitation System.

2. System Frame

The AAL system is illustrated in Figure 2. A high strength aluminum frame supports the levitator structure on a steel table top. Two 250 watt CO₂ heating lasers are mounted on opposite sides of the frame. Levitator and laser electronics are mounted in the frame. Electrical cables pass from the electronics to the levitator components through a hole in the table under the levitator. A Vision Research fast camera and laser hearth melter are mounted on the table top and an “Exactus” optical pyrometer is mounted on the levitator structure.

The back side of the system frame has electronic supplies for the second CO₂ laser. Mounted in the area below the hearth melter are manual laser power controls, gas supply interface, electrical power connections, and an “IOLAN” device server for the digital communications. The device server provides an Ethernet bridge to the desk top computer that operates the system.

Dimensions of the apparatus are given in the plan and elevation views of Figure 3.

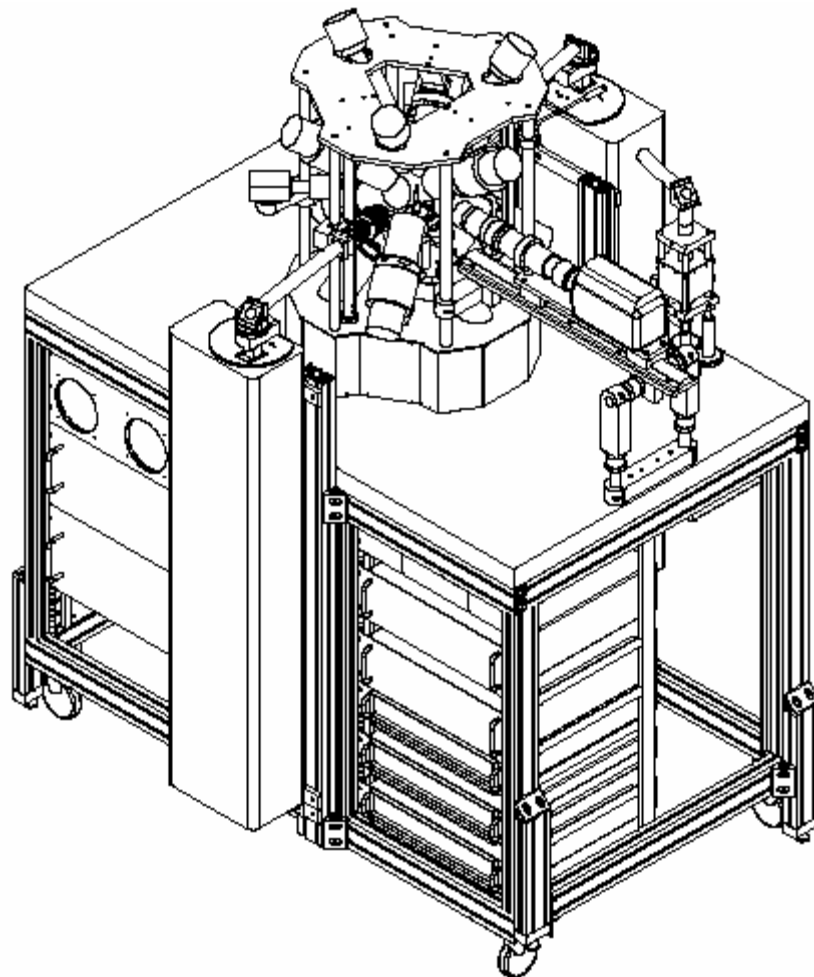


Figure 2 AAL System showing the frame, CO₂ lasers, levitator, electronics and instruments.

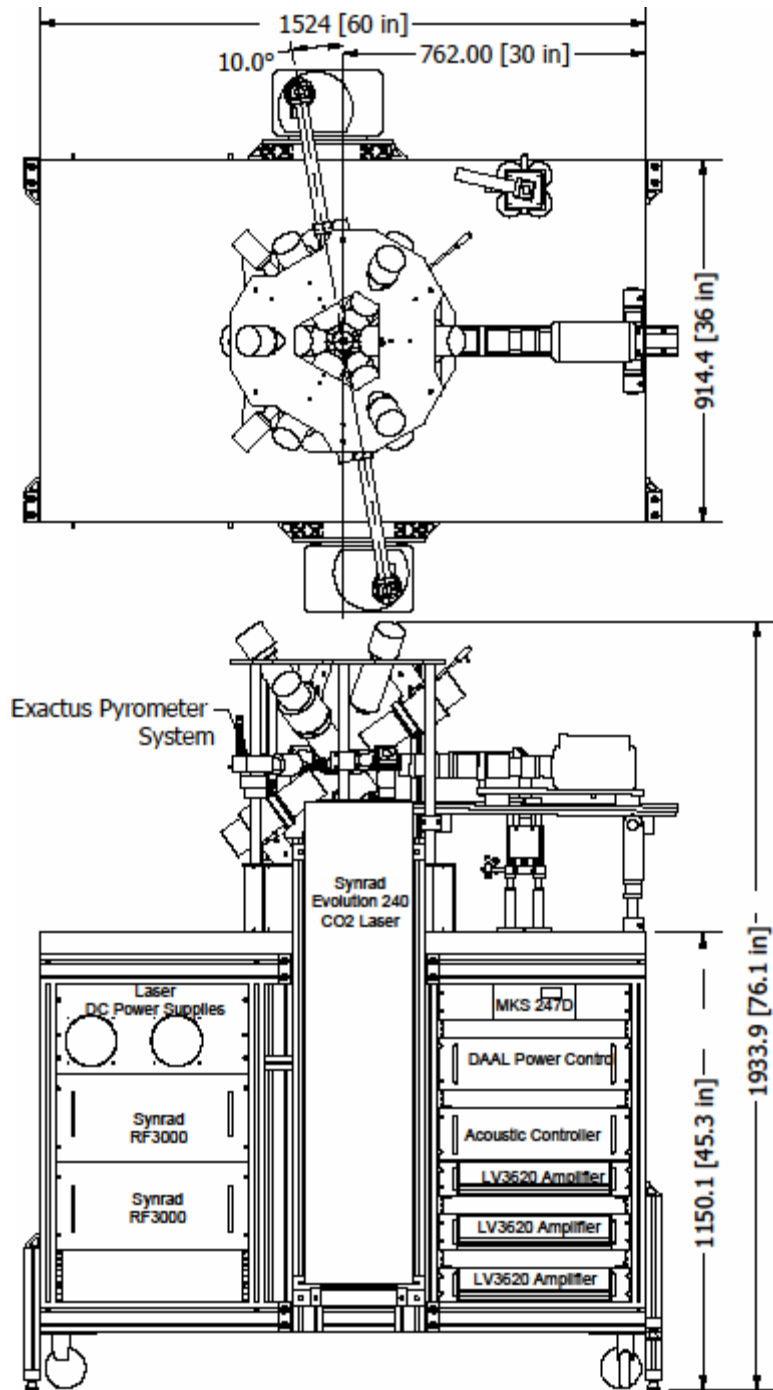



Figure 3 Plan and elevation views of the AAL system with dimensions in mm and inches.

2.1 Par Frame Structure

The AAL system frame is constructed from “TSLOTS” extruded aluminum components. Specifications and a picture of a typical TSLOTS frame component are in Table 1. The TSLOTS components are supplied by Futura Industries, (<http://www.futuraind.com/tslots>).

Table 1 TSLOTS frame specifications.

<p>Alloy – 6063*, T6 Temper Yield Strength – Mpa = 200 0.2% Proof Stress – ksi = 29 Tensile Strength – Mpa – 230 0.2% Proof Stress – ksi = 33 Elasticity (E) – approximately 10,000,000 lbs./sq.in. Hardness – Webster Model "B" 11-12 Flatness – .004" per inch of width Straightness – .0125" per foot of length, not to exceed .120 inches over 20 feet of length Twist – Twist per foot of length does not exceed .25° and total twist over 20 feet of length does not exceed 1.5°</p>	
---	---

2.2 Newport Breadboard AAL Mounting Surface

The top surface of the Par Frame structure is a 3' x 5' (0.90 x 1.50 m) IG-series optical breadboard, from Newport (<http://www.newport.com/>). The center of the breadboard has an 8" (203.2 mm) diameter access hole for connections between the AAL structure and components mounted in the system frame.

Specifications for the Newport breadboard are in Table 2.

Table 2 Newport table specifications.

Working Surface	400 Series ferromagnetic stainless steel 0.134 (3.4 mm) thick with integrated damping layer
Thickness [in. (mm)]	2.3 (58)
Surface Flatness [in. (mm)]	±0.006 (±0.15), over 2 ft (600 mm) square
Core Design	Trussed honeycomb, vertically bonded closed cell construction, 0.010 in. (0.25 mm) Steel sheet materials, 0.030 in. (0.76 mm) triple core interface
Broadband Damping	Integrated Damping including constrained layer core, damped working surface and composite edge finish
Mounting Hole Type	Cut (not rolled) threads with countersink 1/4-20 holes on 1 in. grid (M6-1.0 holes on 25 mm grid), 0.5 in. borders (12.5 mm borders)
Hole/Core Sealing	Easy clean conical cup 0.75 in. (19 mm) deep Non-corrosive high impact polymer material

3. Levitator Structure and Components

The levitator is illustrated in Figure 4. Labeled components are listed in the following table.

Table 3 Levitator components.

Item	Description
1	Levitator frame
2	Geometric centering device
3	6 Acoustic transducers
3a	6 Transducer positioning devices
4a	3 Position sensor laser assemblies
4b	3 Position detector assemblies
5	Gas jet assembly
6	Specimen injector
Not shown: 2 video cameras	

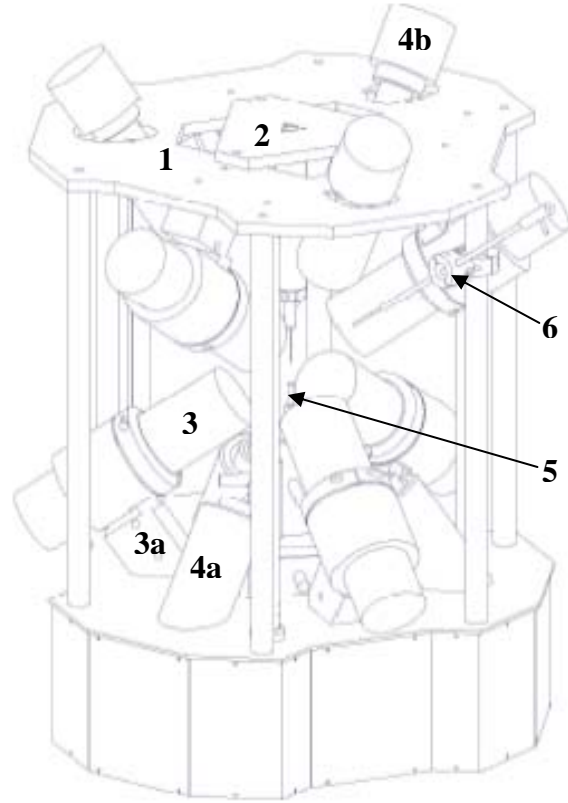


Figure 4 Levitator structure and components.

3.1 Levitator Frame

The levitator components are mounted on two aluminum plates of approximately 22" = 559 mm diameter and separated by 19.750" = 501.65 mm. Below the lower plate is a section that contains electrical wiring and gas flow delivery. Cooling fans and the gas jet heater panel are in the walls of the lower section..

3.2 Centering Device – “Chessman”

When installed in the top plate of the levitator frame, the geometric centering device, dubbed the “chessman”, holds a 3 mm steel ball centered exactly half-way between the upper and lower plates of the levitator. This is the position at which the system components are aligned to levitate samples. The centering device has a triangular mounting plate with holes indexed to holes in the top plate of the levitator. Two video cameras mounted on the levitator frame are adjusted to center images of the ball at marked position on video monitor screens. The video cameras are used for alignment experiments and to observe and control sample position in levitation experiments.

3.3 Acoustic Transducers

Six acoustic transducers, item 3 in Figure 4, are mounted 3-each on the upper and lower aluminum plates. They are supported by transducer positioning devices, item 3a, used in system alignment. The three pairs of opposed sound sources are on orthogonal axes, labeled axes X, Y,

and Z. The sound source pairs create standing waves that exert force on levitated samples. The position of nodes and anti-nodes in the standing waves depends on intra-axis phase differences. Torques on a levitated sample result from inter-axis phase differences. The system has automatic controls of the intra-axis phase differences that stabilize levitation. Operator-adjusted inter-axis phase differences are used control sample rotation.

The sequence of acoustic axes and of transducers mounted on the lower and upper plates of the levitator for the X, Y, and Z axes is clockwise when looking down on the levitator. The X axis is in the same vertical plane as the Vision Research camera.

The photograph in Figure 5 shows internals of the acoustic transducer assembly. The transducers are resonant horns designed to operate in a narrow band at a frequency of approximately 22.2 KHz. The transducer cooling fan is controlled by system software to be on if the resonance frequency is less than the operating frequency. This control makes the resonant frequency of each horn drift towards the operating frequency as the transducers warm-up. The operating frequency is taken equal to the average resonant frequency of the six transducers. The resonant frequencies are calculated from the phase difference between current and voltage in the acoustic power circuits. The “motor” is a set of four piezoelectric rings set in epoxy. The rings are type EC-64, lead zirconate titanate “Hard”, from EDO Corp., now ITT Acoustics Systems.

The photograph shows a ribbon microphone attached to the underside of the horn, which was previously used to monitor the acoustic output signal, or sound pressure level, SPL. These ribbon microphones are no-longer used. SPL is accurately calculated from the electrical power delivered to the transducers, within the range of near-resonant frequencies that occur in levitation experiments.

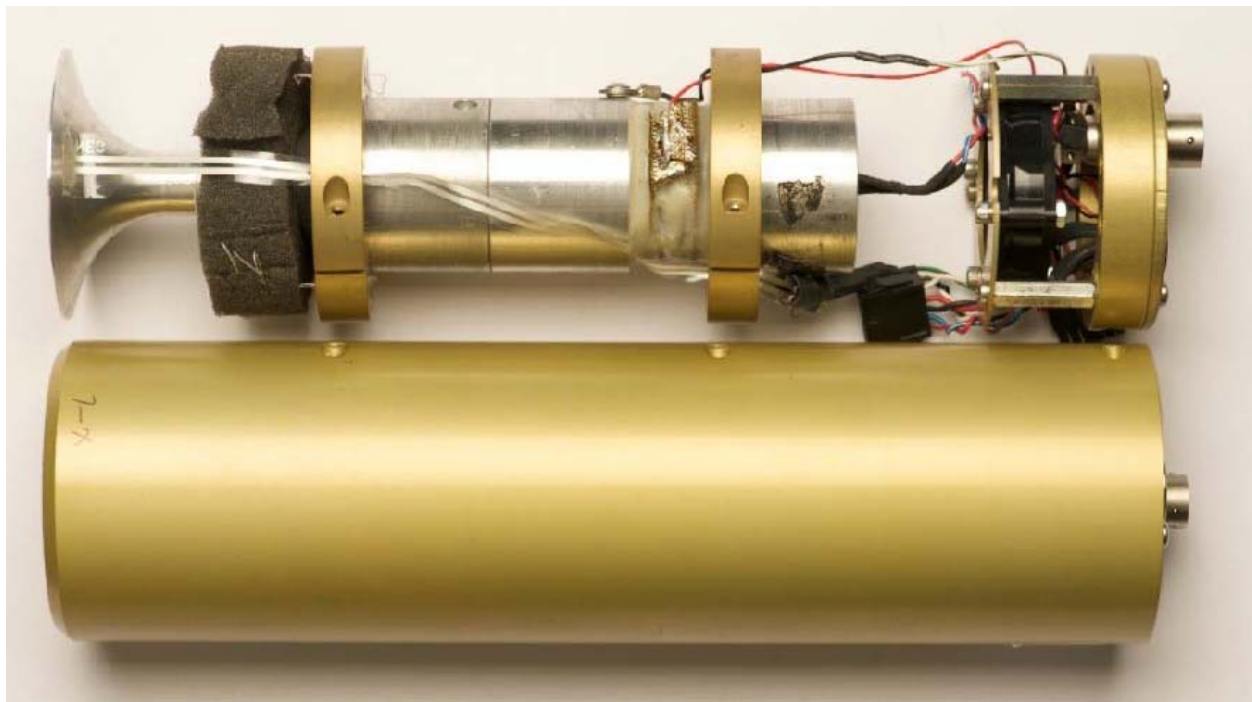


Figure 5 Acoustic transducer

3.4 Position Sensing System

The position sensing system forms a shadow, in 808 nm diode laser light, of the levitated sample on a position sensitive detector. Three laser assemblies, item 4a in figure 4, are mounted on the bottom plate and three position detector assemblies, item 4b, are on the top plate. The position signals from the three sensors control acoustic phases for the three sets of acoustic transducers to dampen sample vibrations. Gimbal mounts in the assemblies are used for system alignment.

The laser diode light source and position sensing detector components are illustrated in Figure 6. The light source is a 70 mw, 808 nm diode laser module, model TECIRL-70G-808 from World Star Technologies, operated at a relatively low output power. The beam is expanded and collimated by a beam expander, model HEBX-4.0-3X-800 from CVI Melles Griot. The diode laser is modulated at a frequency of 40 KHz. An 809 ± 11 nm (half-width) interference filter limits the waveband of light reaching the detector. The received light is spatially-filtered by focusing through a pinhole aperture that passes the diode laser light and rejects most of the incandescent light received by the lens. The detector is a Hamamatsu model S5991-01 two-dimensional position-sensitive detector. The combination of spectral (808 nm), spatial, and temporal (40 KHz) filtering allows position sensing with negligible interference from incandescent sample light at sample temperatures in excess of 3000°C .

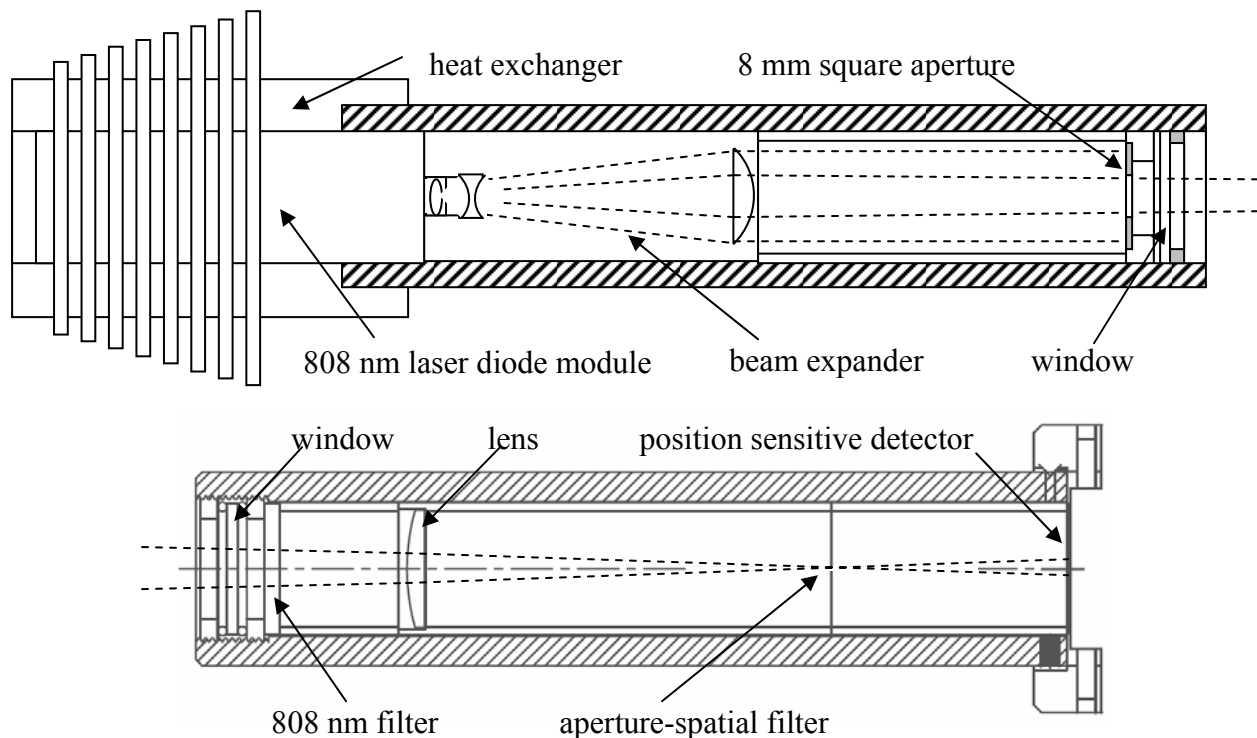


Figure 6 Position sensing system, diode laser source (top) and detector assembly (bottom)

Position detector signals are analyzed by analog and digital electronics to extract the 40 KHz component of the detected signals and produce sum and difference voltages, V_{Ref} and V_Y proportional to the total detected intensity and to the shadow position on the detector. The ratio V_Y/V_{Ref} is used with calibrations to calculate the velocity of the levitated sample. Phase change

instructions at a rate of 250 per second are transmitted to the acoustic controller that to suppress the motion and dampen any oscillation of the levitated sample.

3.5 Gas Jet

The levitated specimen is supported by aerodynamic forces from a heated gas jet that issues from a 0.095" (2.41 mm) inside diameter mullite gas flow tube. The maximum gas flow rate is approximately 300 liters/hour, provided by a 5 liter/min MKS flow controller. The specimen is levitated at a distance approximately 2.5 cm = 1 inch (or less) above the end of the gas flow tube. The gas jet assembly is mounted on a two-axis translation stage centered on the middle plate of the AAL frame. It has height and tilt adjustments. A drawing of the gas jet assembly is given in Figure 7. A photograph of the assembly with a levitated 3 mm sphere is shown in Figure 8.

Illustrated components of the assembly are:

- 1 - mullite flow tube
- 2 - tilt adjustments
- 3 - height adjustment
- 4 - X-Y translation.

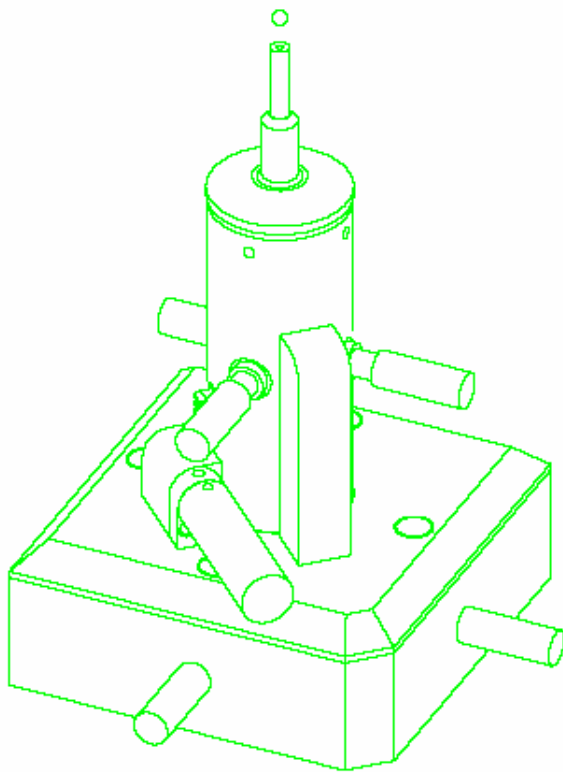


Figure 7 Gas jet assembly.



Figure 8 Photograph of the gas jet assembly.

The MKS flow control transducer is mounted on the levitator frame. It is an MKS Type M100B Mass-Flo Controller, Part Number M100B01353CS1BV. The flow transducer delivers up to 5 standard liters/minute of nitrogen gas, i.e., an amount of gas equal to 5 liters measured at a pressure of 1 bar and a temperature of 0°C. This flow rate equals 5/22.4 of one gram-mole of gas per minute. Calibration factors depend on the heat capacity of individual gases and are given in the MKS operating manual. The flow transducer is controlled and read by an MKS Type 247D Four Channel Readout, Serial Number 016495777. The 4-channel readout device allows expansion of the flow facility by installing additional flow transducers.

(Channel 1 of the Model 247D Readout device failed during system development. Channel 2 is currently used for flow control. Two additional flow controllers operated by Channels 3 and 4 could be added in the future.)

In practice, sample spin control is facilitated by inclining the gas jet approximately 0.1 degree in the vertical plane the X-axis, towards the fast camera. A plumb line and long steel rod inserted in the ceramic tube of the gas jet assembly are used with the gas jet tilt adjustments for this purpose.

Gas flow is manually controlled by the operator in response to observed sample position on the video camera screens. Two gas flow control knobs (fine-left, coarse-right) are integrated with the gas flow controller for the operator's convenience.

Air, oxygen, nitrogen, or argon can be used as the levitation gas. Other gases may also be used, but have not been demonstrated. The gas supply line connects to a 1/8" Swagelok bulkhead fitting on the flow controller panel. A Swagelok particle filter is installed between the bulkhead fitting and the MKS flow controller.

Heating of the levitation gas is used to maintain laminar flow of the gas jet. A resistance heater is used, typically at a heater temperature of 500°C as measured by a type K (chromel-alumel) thermocouple and displayed on the gas jet heater control panel. The heater is a 0.013" (0.32 mm) diameter nichrome wire winding on the mullite flow tube, with an electrical resistance of approximately 35 ohms. A transformer, installed in the AAL power panel reduces the 230 VAC input power to less than 100 VAC delivered to the variac on the heater control panel that supplies power to the heater.

3.6 Specimen Injector

The specimen injector is a "vacuum chuck" connected to a small vacuum pump mounted in the gas heater control panel. The vacuum chuck is an aluminum tube with a ceramic tube at one end that holds the sample and an opening at the other end that can be closed or opened by the operator's thumb. The chuck is inserted into the levitator until the sample is shown on the video screens to be at the levitation position. The sample is then released and the vacuum chuck is withdrawn.

4. Electronic Components

4.1 Acoustic Amplifiers.

Three stereo amplifiers, AE Techron model LV3620, mounted in the system frame drive the six acoustic transducers. The amplifier outputs are controlled by preamplifier signals from the acoustic controller, at equal frequencies and AC voltages, V , and phases. The acoustic controller also measures the output current, I , and the phase difference between electrical currents and voltages for each transducer. Voltages are varied to keep the acoustic outputs constant as the I-V phase difference and amplifier output current vary with the difference between resonance and operating frequencies.

4.2 Acoustic Controller

The acoustic controller is mounted in the system frame, above the three acoustic amplifiers. The acoustic controller sets the frequency, phase, and voltage outputs of the acoustic amplifiers in response to instructions from the operator's desk-top computer and position sensor signals. It measures the amplifier output currents and current-voltage phase differences and transmits these measurements to the desk-top computer. The desk-top computer returns voltage and frequency values to the acoustic controller to maintain the output acoustic frequency at the average resonant frequency of the six transducers and the transducer SPL at the operator-selected value.

The acoustic controller also determines, as manually set on the desk-top computer, the phase differences between the pairs of transducers for the three acoustic axes, and the phase differences between the three pairs of transducers. The intra-axis phase differences determine the position of acoustic positioning forces on a levitated sample. The inter-axis phase differences control sample rotation. The acoustic positioning forces automatically respond to signals from the position sensors to dampen sample position oscillations and control the influence of sample shape change during melting operations.

The acoustic controller is mounted on slides and can be pulled out from the rack-mount to access connectors used for oscilloscope measurements of the amplifier voltage and current outputs. Figure 9 is a top view of the instrument in its pulled-out position. The current/voltage terminals are at the top. From the left side of the picture, the current terminal is first and the voltage terminal second for each of the six channels. Oscilloscope probes are supplied for such measurements. The voltage values are from 0-200 volts measured with a 10:1 voltage probe. Current values are typically 0-1.5 volt, as measured across 1 ohm resistors.

Figure 9 also shows the 7 electronic boards of the acoustic controller and a ± 12 VDC power supply that supplies power to the boards. From the left, the first board is for communications purposes. The next six boards control the acoustic transducers for acoustic axes X, Y, and Z. The order is, XA, XB, YA, YB, ZA, ZB, where the letter "A" designates transducers mounted on the lower plate of the levitator and "B" is for the upper plate.



Figure 9 Interior of the acoustic controller.

The power supply and electronic boards of the acoustic controller are located in a self-contained module that can be removed from the rack-mounted enclosure, for service or replacement of boards, components, or the entire module.

Photographs of the communication and acoustic control boards are given in Figure 10. The circuit cards are identical but the circuits differ, as determined by positions filled or not filled with components on the different boards.

4.3 Sensor Detector Electronics

The detector electronics are built-in to the sensor system structure. Each of the three position sensing axes is perpendicular to the acoustic axis influenced by the sensor signals. The sensors detect light from 808 nm diode lasers operated at 40 KHz that cast a shadow of the levitated sample on the detector. The detector yields four signals that are resolved into a difference signal proportional to the position of the shadow and a sum signal proportional to the total intensity. An analog circuit produces the sum and difference signals and supplies them to a digital circuit that measures the AC component of the two signals. The ratio of the difference and sum signals is calculated and its rate of change determined. The digital circuit is programmed to transmit a phase change signal to the acoustic controller that is proportional to the velocity of sample motion. These signals are instructions sent at a frequency of 250 per second to change the acoustic phase of the transducers so that acoustic forces will reverse the direction of sample velocity. Gain in the feedback control of sample oscillation is set by the operator.

Photographs of the analog and digital boards of the sensor system are given in Figure 11. The analog boards have two potentiometers that control gain in the circuits that provide the difference and sum signals. These pots are the blue-colored devices on the board.

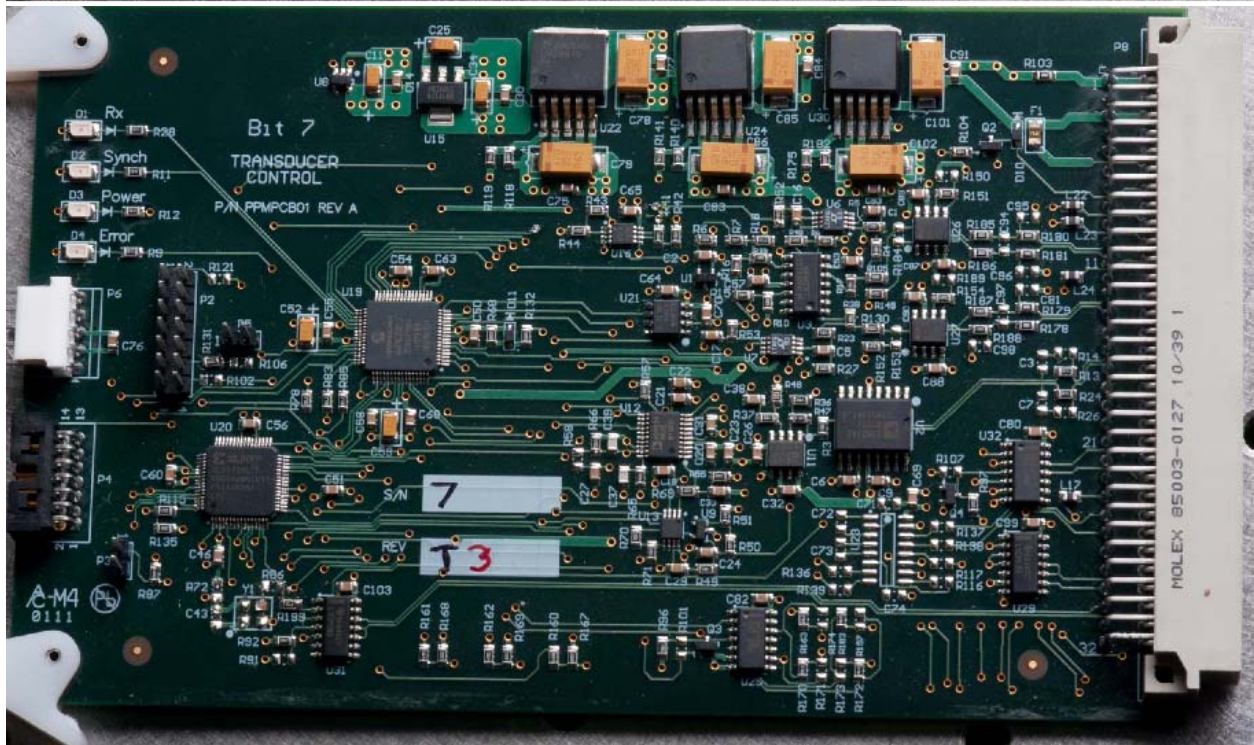
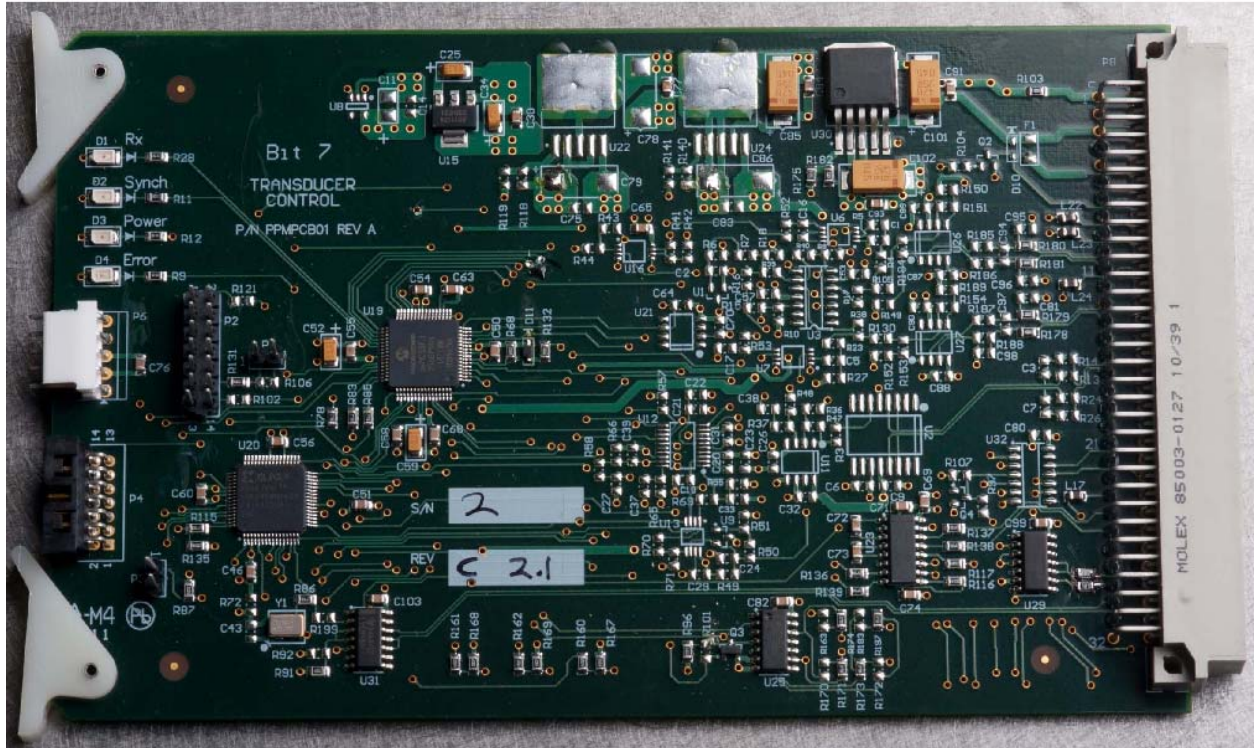


Figure 10 Acoustic controller circuits: communication top, transducer control bottom.

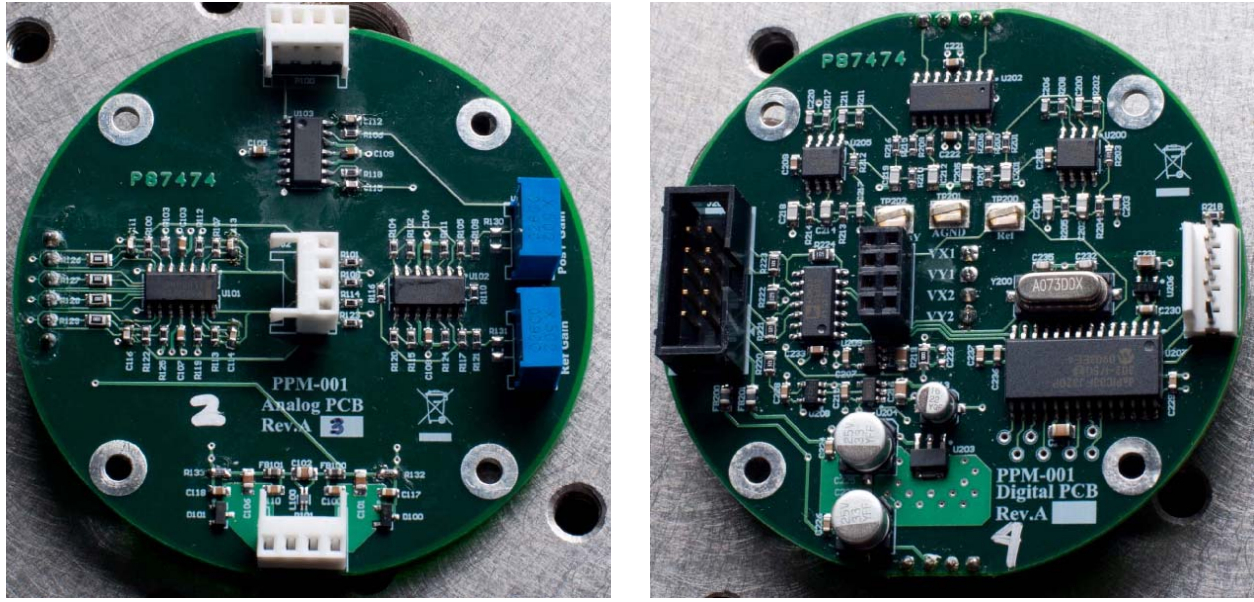


Figure 11 Sensor electronics: analog left, digital right.

4.4 Power Panel

The power panel is mounted in the system frame above the acoustic controller. The front of the Power Panel is shown in Figure 12. The power panel supplies AC and DC power to the following components of the system.

- Three sensor systems:
 - ± 12 VDC to the detector electronics.
 - + 3.3 VDC to the diode lasers.
 - + 12 VDC to diode laser cooling fans.
- 12 VDC to two video cameras mounted on the levitator frame.
- Aux 12 V DC1 for gas flow control.
- Aux 12 V DC2, spare DC supply.
- 12 VDC to the Vacuum chuck pump.
- DC power, via AC/DC power adapters to:
 - Vision Research fast camera
 - Zaber translators for the pyrometer (Aux AC).
 - Exactus pyrometer.
 - 2 Synrad CO₂ laser controllers.
- AC power to the thermocouple gage temperature monitor.
- AC power via a 3.3:1 step down transformer to the gas jet heater control panel.



Figure 12 AAL power panel.

4.5 MKS Gas Flow Controller

The MKS Type 247D Four Channel Readout device is installed at the top of the system frame, above the Power Panel. It operates a 5 liter/minute MKS Type M100B Mass-Flo Controller mounted on the opposite side of the frame. The first channel of the readout device failed during development. The second channel is now used for flow control. The remaining channels of the readout device can be used to expand the gas delivery system for operation with several different gases. Coarse and fine potentiometer controls are added adjacent to the readout device for convenient use by the operator for flow control during levitation experiments.

4.6 IOLAN Device Server

A Perle Systems, Ltd. IOLAN model Rack Mount device server, part number 5500173-13 is installed in the system frame opposite the acoustic electronics and controls. It provides Ethernet connection to serial communication devices of the AAL system.

4.7 Electrical Supply Lines

Two 240 AC, 30 ampere, single phase AC lines are required for the levitator electronics. One line supplies the three acoustic transducers. The second line powers the Acoustic Controller, the Power Panel, the MKS flow controller, and the IOLAN device server.

The AAL system includes a video monitor/recorder and a desk-top computer that have wall-plug power connections.

4.8 Synrad CO₂ Laser Electronics

Each laser has two model RF3000 power supplies operated from two Model DC-100 power supplies. Four 240 volt 30 amp single phase inputs are required, one for each of the four DC power supplies. Each laser has a model UC2000 laser power controller that can be selected for manual operation at the controller knob or remote operation by instructions from the desk-top computer.

5. Instruments

5.1 Video Cameras

Two video cameras (Figure 13) are mounted on the levitator frame to observe levitated samples from approximately orthogonal directions in the horizontal plane. Their mounts can be adjusted to increase their angular separation to approximately 110° so that the two cameras are nearly in the vertical planes of the Y-axis and Z-axis acoustic transducers. The cameras are Watec, model WAT-902H2 ULTIMATE monochrome CCD cameras. Components marked in the figure are: A–Watec video camera, B–Computar auto-iris lens, C–Variable neutral density filter.

Computar model TG10Z0513FCS-2 auto-iris lens are mounted on the cameras. The auto-iris capability of the lens is not sufficient for the large range of sample intensities encountered in heating experiments. A 5 mm extension tube is mounted on each lens that integrates a variable neutral density filter for further control of image intensity.

5.2 Video Recorder - Monitor

The video camera images and the output of the Vision Research camera are displayed on a 4-screen video monitor, Figure 14. The CO₂ laser cut-off switch is shown in the foreground of the figure. Images from cameras V1 and V2 are in the upper left and lower right quadrants of the monitor. The images are recorded on a 500 GB hard disk that retains several hundred hours of

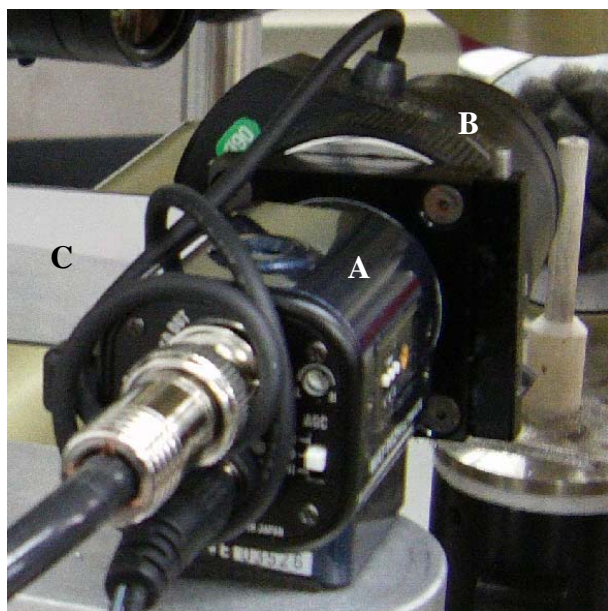


Figure 13 Video camera, lens, neutral density filter.

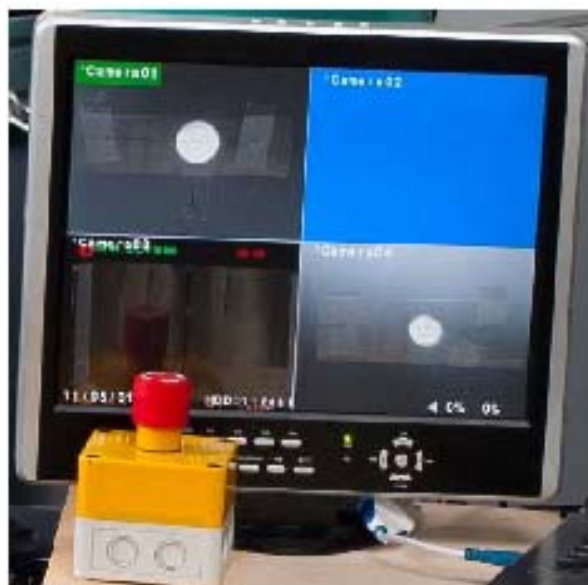


Figure 14 Video monitor and laser cut-off switch.

recording at 30 images/second. Recorded images can be displayed, searched, and transmitted through a USB port. The video monitor has wall plug power connection and is typically located at the operator's desk or placed on the levitator top surface.

The disk storage device of the video monitor failed and was replaced during system development. It is Western Digital (www.westerndigital.com) product, Model WD5000AVVS-63M8BO.

Transparent sheets marked to indicate the optimum levitation position are attached to the monitor. The transparent sheets are positioned in alignment experiments using the "chessman" alignment tool.

5.3 Vision Research Fast Camera and Infinity Lens

The fast camera, lens, and support structure are illustrated in Figure 15. The camera is model Phantom V9.1 from Vision Research, Inc. It provides up to 14-bit image depth, and 1,000 frames per second at a full resolution of 1,632 x 1,200 pixels. Faster measurements are possible at reduced resolution. The camera has 6 GB of memory, sufficient for 3.19 seconds of continuous full-format recording at 1,000 frames/second and 8 bit image depth. The lens is an Infinity model K2SC long-distance microscope lens with model CF-2 objective. The camera/lens system can acquire near full-screen images of levitated 3 mm diameter samples.

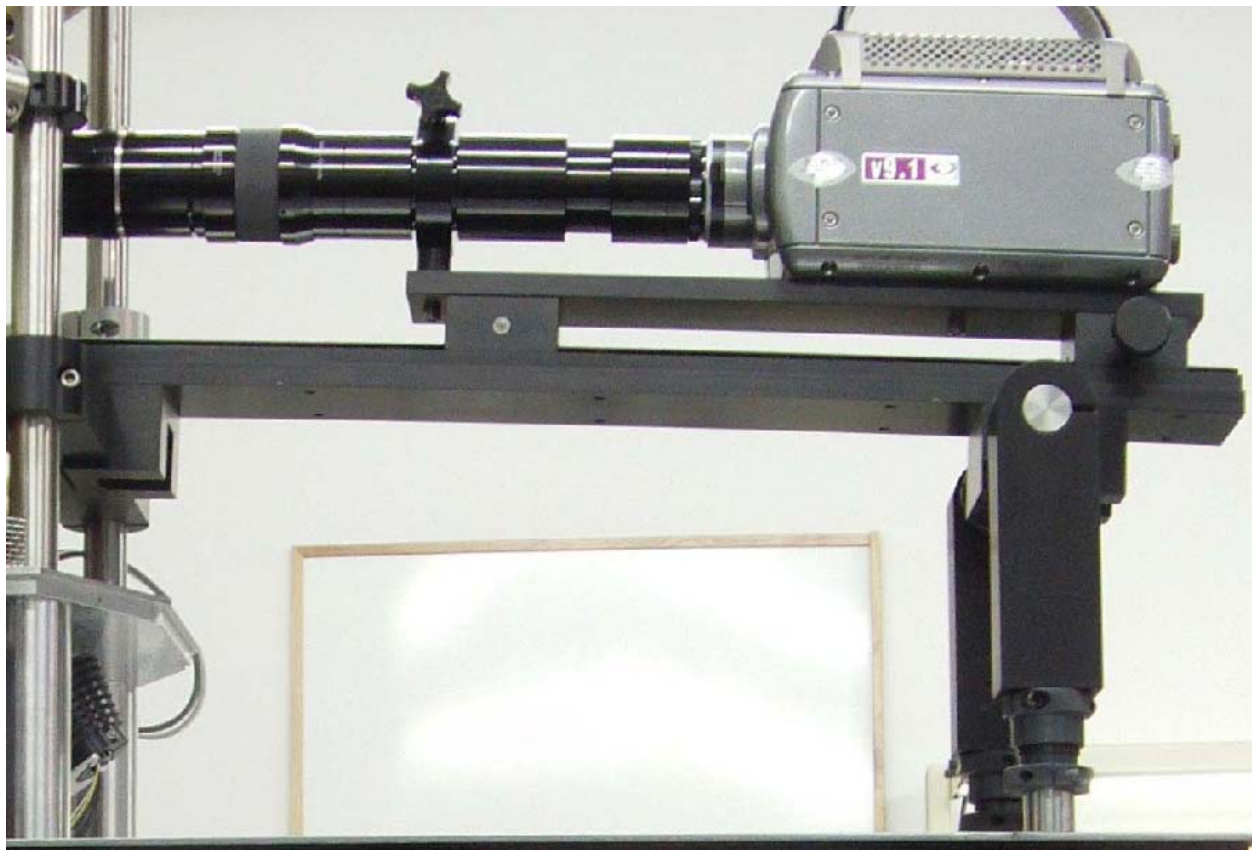


Figure 15 Vision Research camera and Infinity long distance microscope lens.

Detailed information about the camera and lens is at:

<http://www.visionresearch.com/Products/High-Speed-Cameras/v91/>

<http://www.infinity-usa.com/products.aspx>

5.4 Exactus Pyrometer

Temperature measurements are obtained with an Exactus model EX-S-1PY-ECS pyrometer, from BASF Corporation, Fremont, California. Pyrometer specifications are given in Table 4.

Table 4 Exactus pyrometer specifications,

Temperature Range	700°C to 3500°C
Spot Size*	0.67 mm
Measurement wavelength	650 nm
Measuring distance	150 mm (from front of pyrometer lens)
Measuring speed	Up to 1000 Hz
Accuracy, T < 2600°C	± 1.5°C or ± 0.15% of measured temperature

* 90% of the signal is within a 0.67mm spot, 99% is within 0.73mm, and 99.9% of the signal is within a 1.0mm spot.

The pyrometer and its positioning equipment, Figure 16, are attached to the levitator frame at a position opposite the Vision Research camera. The positioning is by a Zaber model LS13E Motorized X-Y Stage with 13 mm travel per axis. Marked components in Figure 16 are: A–pyrometer, B–horizontal positioner, C–vertical positioner, D–manual control knob.

The Exactus Pyrometer Screen of the graphical user interface (see section 5.8.4) allows the operator to plot horizontal and vertical temperature scans across the levitated sample. The results of the temperature scans are used by the operator to specify the position at which temperature

is measured on a levitated sample.

A green diode laser pointer fits onto the pyrometer to identify the exact spot on levitated samples at which measurements are obtained.

5.5 Gas Heater Control

The gas jet heater control is located in the base of the levitator structure. It includes a variac for control of the power delivered to the gas jet heater and a thermocouple monitor that reports the

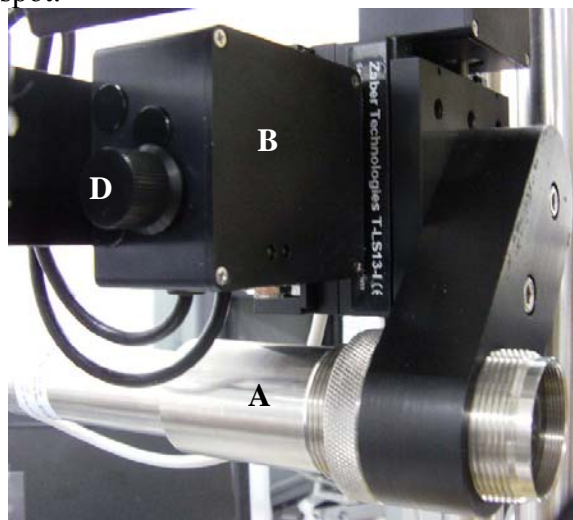


Figure 16 Exactus pyrometer and positioning device.

gas jet heater temperature. The temperature is measured by a type K thermocouple (Ni-Cr vs Ni-Al) and monitored by a model DP63300-TC panel meter from Omega Engineering, Inc., <http://www.omega.com/>. The variac setting is approximately 80% for a heater temperature equal to 500°C with a gas flow rate of 3 liters/minute of nitrogen gas.

5.6 Laser Hearth Melter

The laser hearth melter (Figure 17) is used to melt powders and prepare dense spheroid samples suitable for levitation experiments. One of the CO₂ laser beams is redirected from the levitator to the hearth melter and delivered vertically down onto powdered materials placed in the copper hearth. The hearth is cooled by contact with its water-cooled support plate. It has handles on either side for the operator. A neutral density filter swings up in front of the hearth for viewing bright incandescent samples.

Re-alignment of the CO₂ laser beam, using the mirror tilt stages is necessary when the beam is switched to and from the hearth melter.

The hearth is cooled by water flow from the cooling water supply for the CO₂ laser that is not used for melting samples in the hearth. A water-flow valve on the hearth melter is opened for hearth melting experiments and closed when the hearth is not in use.

Samples of hearth melted oxides are pictured in Figure 18. From left to right, the materials are: ZrO₂/20%Y₂O₃, Gd₂Zr₂O₇, ZrSiO₄. The ZrO₂/20%Y₂O₃ material did not form spheroid melts, due to a low value of the liquid surface tension.

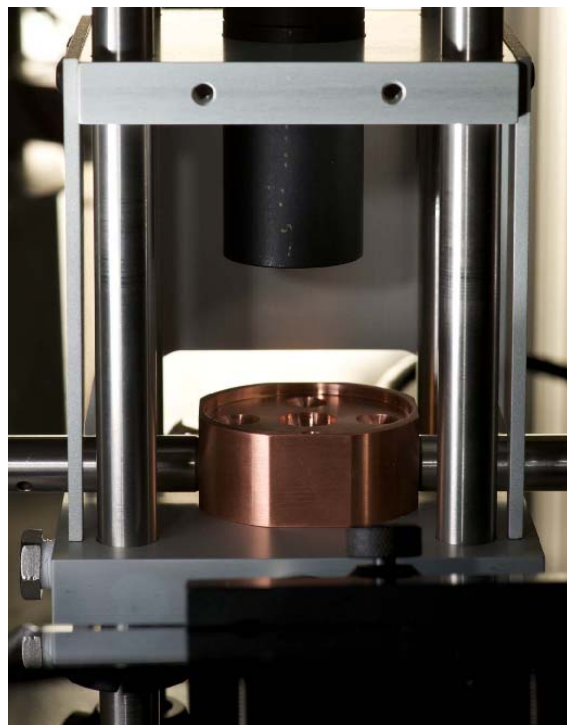


Figure 17 Laser hearth melter for sample preparation.



Figure 18 Hearth-melted oxides.

A hearth-melting experiment performed on $ZrSiO_4$ resulted in undercooling and rapid crystallization of a part of the sample when laser heating was turned off. Figure 19 illustrates the dendrite microstructure of this material.

Hearth melting experiments¹ have demonstrated negligible contamination of oxide materials melted in the hearth.

¹ J.K.R. Weber, J.J. Felten, and P.C. Nordine, "Laser hearth melt processing of ceramic materials," *Rev. Sci. Instrum.* **67** (2) February 1996, pp. 522-524.

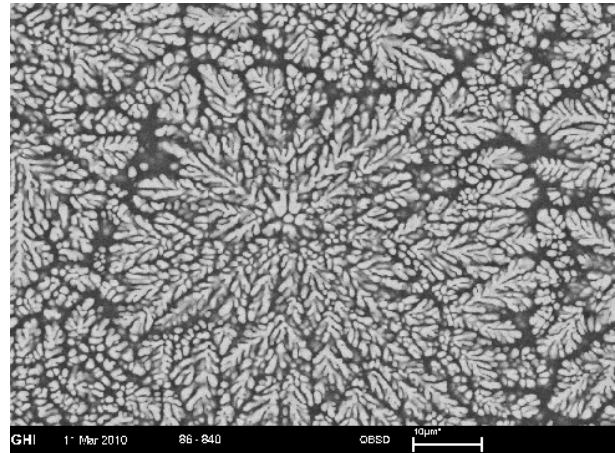


Figure 19 Microstructure of $ZrSiO_4$ formed in the laser hearth melter.

5.7 CO_2 Lasers

The AAL system has 2 Synrad model Evolution 240 CO_2 lasers mounted vertically on opposite sides of the system frame. Figure 20 shows the laser beam delivery system. The vertical output of the lasers (1) is directed by molybdenum mirrors and tilt-stages (3) to nearly horizontal beams aimed at opposite sides of levitated samples. The beams are pointed slightly downward, so that the end of the delivery tube for one laser serves as a beam stop for the opposite laser.



Figure 20 CO_2 laser beam delivery assembly.

A diode laser accessory (2) mounted at the top of the laser can be turned on by its switch, to provide a red beam in place of the invisible CO_2 laser beam with which the red beam is aligned. This visible beam assists in laser alignment. Final alignment with a levitated sample is obtained by operating the tilt stage while observing the temperature of a beam heated sample. This alignment operation is best performed at a relatively high sample temperature (typically $1500^\circ C$) to obtain a small thermal response time.

Item 4 marked on Figure 20 has 125 mm focal length ZnSe lens in a sliding mount, for adjusting the beam diameter at the sample. The CO_2 laser beam divergence of 3.2 mr (0.18°) puts the laser

beam diameter equal to 5.9 mm at the lens and the focal point at 134 mm from the lens. With the lens in the forward and back positions, the laser beam diameter at the levitated sample is then equal to 3.8 and 6.4 mm, respectively. Moving the lens forward puts a larger fraction of the laser power on the sample but also increases temperature gradients in the sample. Temperatures in excess of 3000°C have been obtained on levitated oxide samples with the lens in the back position.

Power for each of the CO₂ lasers is from two Synrad model DC-100 and RF3000 power supplies. Two 30 amp, 240 Volt single phase (or 3 phase) circuits supply each laser. Each laser requires cooling water at a flow rate up to 4 gallons/minute, 15.1 liters/minute.

The lasers are operated by Synrad UC2000 laser power controllers, either manually, or via the laser control screen of the graphical user interface. An emergency shut-off switch (see Figure 14) is provided at the operator's desk. The laser shut-down circuit has added connections for shut-off switches that may be installed by a client.

5.8 Graphical User Interface, GUI

The graphical user interface (GUI) is presented on the monitor of the desk-top computer. The GUI reports values of AAL system operating parameters and is used by the operator to control the instrument. It has five separate screens, the AAL Console, Sensors, Laser Power, Exactus Pyrometer, and Scope screens. All but the Scope screen come on when the system is started and the password entered. The Scope screen is raised by selecting "Scope" on the AAL Console screen.

5.8.1 AAL Console Screen

The AAL Console screen, Figure 21, presents operator controls for the six acoustic transducers, 2 each on the X, Y, and Z acoustic axes. It controls the sound pressure level (SPL), the relative acoustic phases of opposed transducers on each axis, and the inter-axis phase differences (spin phases) that influence acoustic torques on levitated specimens. The screen reports the resonant frequencies of each transducer, which vary slightly when operated due to transducer temperature changes with time when the SPL is changed and by heat transfer from levitated samples. The operating frequency is equal to the average of the six resonant frequencies. The AAL console can modulate the intensity of one or more acoustic transducers, at specified frequencies. The modulation capability is applicable in studies the oscillation behavior of levitated liquids from which values may be determined for the liquid surface tension and viscosity.

5.8.2 AAL Sensors Screen

The AAL Sensors screen, Figure 22, provides operator control of the gain values used for feedback from the sensor system to the acoustic controller. The sensor system derives the velocity of sample motion along the X, Y, and Z acoustic axes. It sends change in phase instructions to the acoustic controller to oppose sample motion by changing the position of the acoustic node in which the sample is levitated. The gain value that determines the magnitude of the phase change is set by the operator to optimize feedback for the sample of interest.

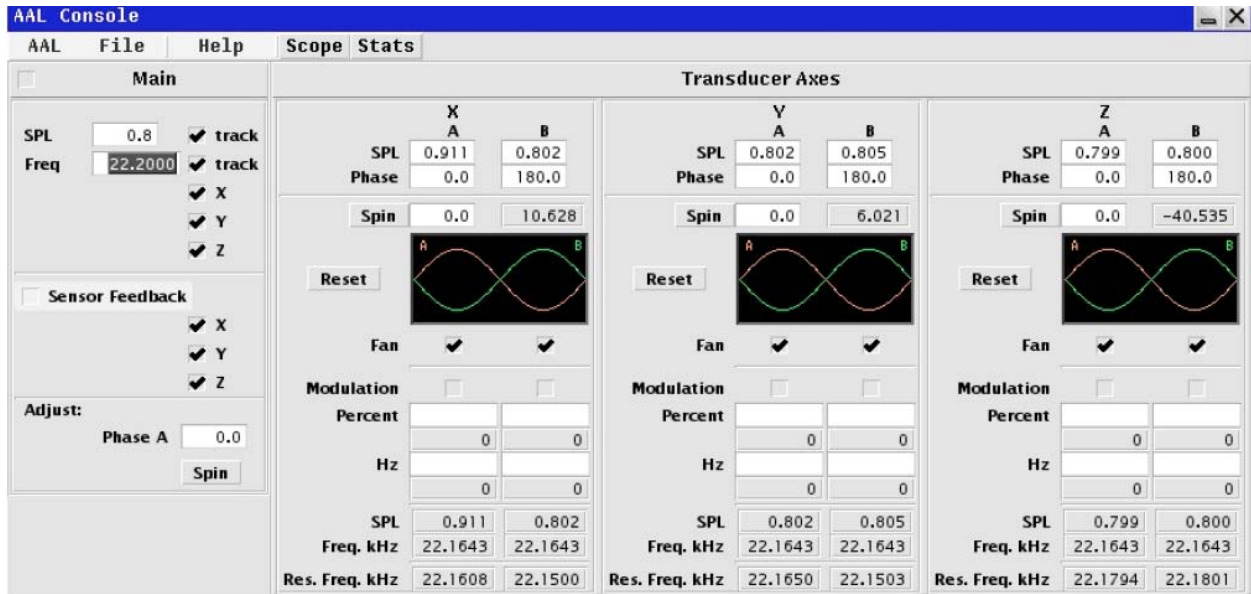


Figure 21 AAL console screen.

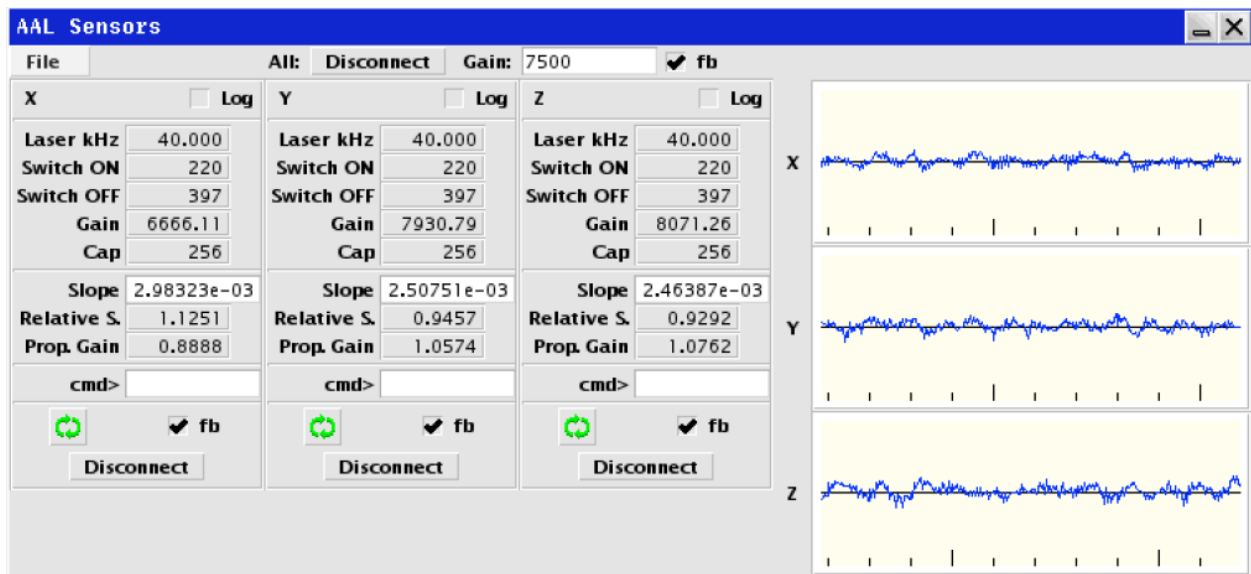


Figure 22 AAL sensor screen.

Slight differences in the sensitivity of the sensor system to sample motion exist for the X, Y, and Z axes. Calibrations determine these differences and are programmed into the system as the “Slope” values stated in the screen.

The Sensors screen includes a real-time graphical display of the sensor outputs for periods of one second.

Sensor feedback is initiated as follows. First check the “connect” box at the top of the screen, or individual “connect” box(es) for each axis. Then enter a feedback gain value, typically in the

range 5000 to 7500. Finally click the “fb” box at the top of the screen or individual “fb” box(es) for the axes. This initiates the graphical displays and sends feedback information to the acoustic controller. For the controller to act on this information, “Sensor feedback” must be checked on the AAL console screen. Feedback information is recorded in a file on the computer disk if the “log” boxes are checked on the sensor screen.

5.8.3 AAL Laser Power Screen

Figure 23 shows the AAL Laser power screen. The UC-2000 Laser power controller’s selection is set to “REMOTE” to enable software control of laser power via the laser power screen. Otherwise “MANUAL” is selected for control via the knobs on the laser power controller.

The lasers to be operated are selected by clicking the upper square buttons on the Laser power screen from grey to green. Clicking “1”, “2”, or “LASE” from grey to red turns laser 1, 2, or both lasers on at the selected percentages of full power output. The two lasers are operated at the same power via the central “B” slide or typed-in power setting. Or each laser can be independently controlled via its slide and power setting panel.

If the mouse is clicked on power to one or both lasers, the top edge of the laser power panel is blue. Then the up and down arrow keys on the keyboard change laser power by +0.5% or -0.5%, respectively, and the page-up and page-down keys change laser power by $\pm 5\%$. Holding the controls on produces repeat changes in laser power with short delays between each power increment.

5.8.4 Exactus Pyrometer Screen

Controls on the AAL Exactus Pyrometer screen are shown on the left side of Figure 24. The right side of the figure shows typical X- and Y-scans of the pyrometer temperature measurement over the surface of a levitated sample. New X-Y scans are generated each time the X and Y buttons are selected by the operator. Older scans remain on the screen until deleted by the operator.

The pyrometer screen controls the Zaber 2-axis pyrometer positioning hardware, according to the X and Y values and scan region selected at the screen. The vertical center line for each scan is automatically at the X or Y position selected on the screen. The scans allow the operator to position the pyrometer at the center, or other selected position on the levitated sample.

The rate of the X-Y scans depends on the temperature acquisition rate. An acquisition rate of 50 to 100 Hz is recommended to keep the scan time within a few seconds.

The dark square in the center-top of the pyrometer screen represents the full 13 mm range of the Zaber 2-axis positioning system. The place within this range designated by the scan region and X, Y selections is marked by the five points within the square. The center point can be adjusted using the mouse if the L/U button is set to U (unlocked). Clicking “Chessman” restores a previous X, Y position that was recorded by clicking “Save” under the File menu. (The “Chessman” name is based on the device used for physical alignment of the AAL components.)

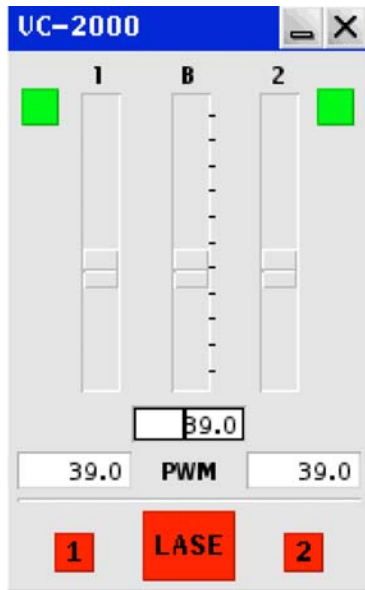


Figure 23 Laser power screen.

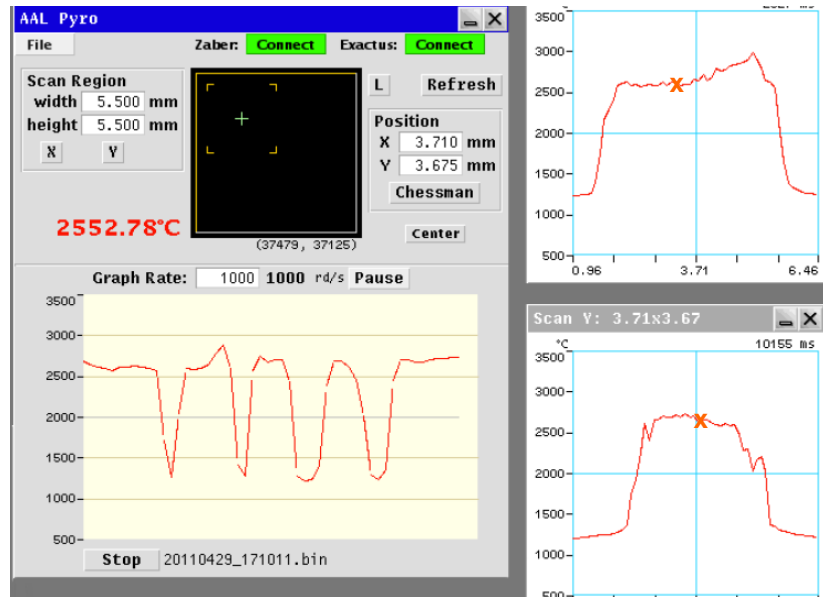


Figure 24 Exactus pyrometer screen.

Clicking “Center” sends the Zaber positioning system to the center of its range. “Refresh” is used at start-up to update the indicated position values to the actual position of the pyrometer. The pyrometer position can also be set by clicking on the temperature line of scans, as indicated by the orange X’s on the scans shown in Figure 24.

The pyrometer screen also controls and displays acquisition of temperature vs time data. The acquisition rate is selected in the middle of the screen and acquisition is started or stopped by the “start/stop” button at the bottom of the screen. The file name in which data are stored is given next to the start/stop selection. The temperature-time data file name is automatically set to equal the current date and start time and stored at /usr/home/aaladm/logs/aal/pyro/file-name.bin.

The temperature vs time graph on the pyrometer screen displays the data obtained during the previous one-minute period. The “pause” button stops the graph so that the operator can examine data of interest, while logging to the data file continues. The graph returns to current data by clicking “pause” again.

5.8.5 AAL Scope Screen

The AAL Scope screen, Figure 25, tracks the current (red sine waves) and voltage (black sine waves) for the six transducers and the inter-axis phase differences that influence sample spin. The phase of the current in the amplifier/transducer circuit varies relative to the voltage in a manner that depends on the transducer’s resonant frequency and the applied acoustic frequency. The phase measurements thus provide a means to follow the resonant frequency of the transducers that are presented on the AAL Console screen.

The left side of the Scope screen illustrates the phase differences between the three acoustic axes that are set by the Spin controls.

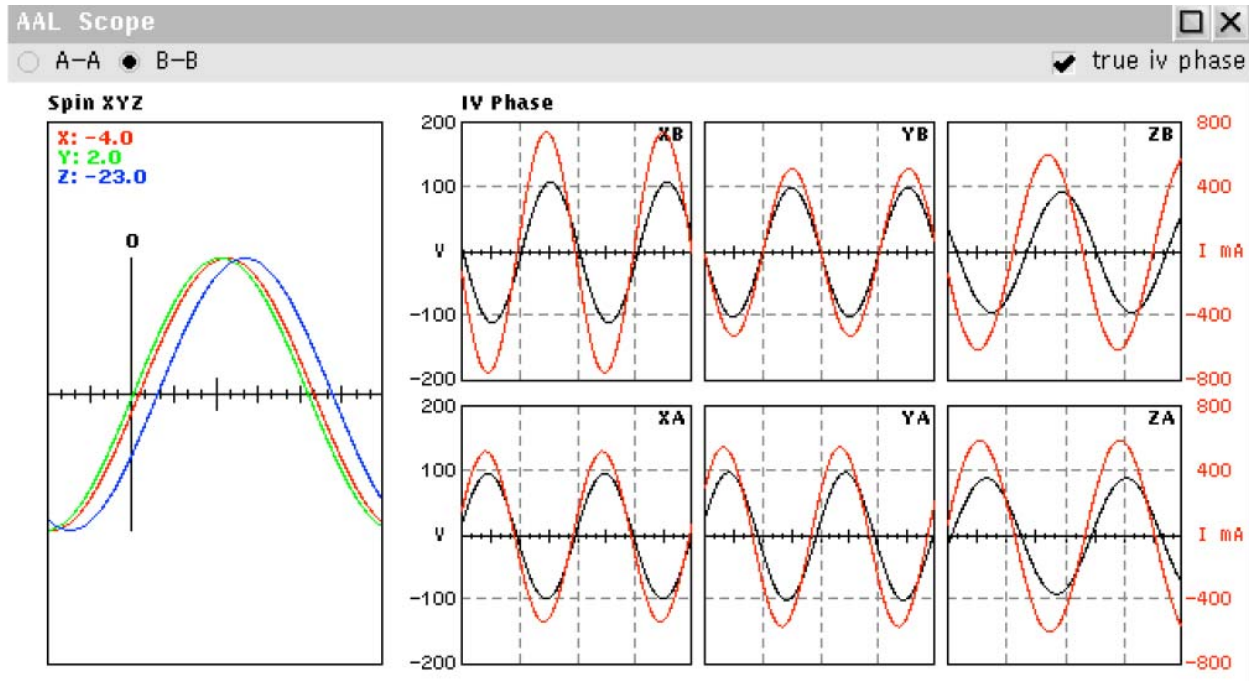


Figure 25 AAL scope screen.

5.9 Computer and Software

The computer is a Lenovo ThinkStation, DE10 Series. It has two monitors, one for the GUI and additional AAL programs under the Linux operating system. The second monitor is typically used under the Windows operating system with the Phantom camera software for the Vision Research fast camera or with the Exactus pyrometer software. The Lenovo has a dedicated Ethernet card for the Vision Research camera to allow rapid downloading of the large video files that the camera records. The computer has a 250 GB SATA drive. Users will need to download Vision Research camera video files to other storage media from time to time.

Operation of both the Phantom software and the AAL software at the same time creates opportunities for keyboard and mouse errors, if the mouse is on one screen and the operator attempts to change parameters on the other screen. Therefore it would be advantageous if users provided a second computer with large capacity and rapid download capability for operating the high speed camera. This would have the further advantage that two operators, one for the AAL and one for the camera can better perform closely timed operations in experiments with precise timing requirements.

The AAL is started-up when the computer is turned on, the password entered, and the operator clicks the first icon below. This opens the AAL console, sensor, laser control and pyrometer screens. The scope screen may be opened by clicking “scope” on the AAL console.

To start-up the Vision Research camera, first click the second icon below. This raises the VMWare screen. Drag the screen to the second monitor and click the green arrow on the left column of the screen to start or resume Windows XP for operating the Vision Research software. The Windows desk appears and the Phantom camera is software initiated by clicking its icon on the desk top or the start menu.



The first time that Windows is started each day requires entry of the password.

AAL operations with levitated and heated samples that use the GUI are discussed later in this manual. The software is detailed in the Programmer's Manual. Separate manuals are provided for the Vision Research camera and the Exactus pyrometer.

In addition to the GUI-based operations, AAL software supports calibration experiments, entry of calibration constants, and data acquisition and storage discussed in the following subsections.

The additional AAL software is implemented through the command shell raised with the Inferno Icon. The Programmer's Manual details instructions that are possible with the command shell. Many of the operations performed by the GUI can also be performed using instructions via the command shell.

5.9.1 Sensor Sensitivity Scans

These experiments are performed at ambient temperature, using acoustic levitation alone. A Styrofoam ball is acoustically levitated by operating all six transducers at an SPL value, typically 0.65 that produces stable levitation.

The recommended procedure for operating the program is as follows.

Start the inferno shell from the launch bar icon to obtain the command window. Create a new directory (called "current date" below) under the tests directory. Enter the instructions:

```
cd tests  
mkdir current date  
cd current date  
aal/sensor/pscheck -a -r 200 -Y
```

This will operate the program and provide feedback information to the operator on the command window while the experiment is in progress.

Data will be stored in the created directory. One file with outputs of the three sensors as a function of the phase values for each of the X, Y, and Z axis sweeps.

Once the experiment is completed, further instructions reduce the data. Entries on the Linux terminal (brought up in the applications menu) are:

```
cd ~/tests/current date  
ln ../scripts/m* .  
ln ../scripts/*.g .  
9 mk
```

This generates a series of pdf files that show the calibration results..

The Programmer's Manual can be referenced for pscheck documentation.

When the sensor sensitivity program is operated, the phase of transducer A for a given axis is swept from -200 to $+200^\circ$ while holding transducer A for the other two axes at 0° and transducers B at 180° . The procedure is repeated to scan the phase of transducer A for axes X, Y, and Z. This operation causes the Styrofoam ball to be moved along each axis from approximately 4.4 mm below the nominal levitation position to 4.4 mm above that position.

The position detector sum and difference outputs, V_{Ref} and V_Y , are simultaneous recorded for all three sensors and the scans for each axis. Later analysis of the recorded data provides position sensing sensitivities for the three acoustic axes, i.e., the rate at which the ratio, V_Y/V_{Ref} , varies with the phase of transducer A.

5.9.2 Transducer Electrical Characteristics

The purpose of these experiments is to determine the relationship between the computerized measurements of transducer voltage, current, and V-I phase difference and the actual value of the properties in units of volts, amps, and degrees.

The measurements are obtained by connecting an oscilloscope to the voltage and current taps for a given channel. The V, I, and phase values measured with the scope are recorded along with those automatically acquired by the computer. The program for making the computer operations is started by entering the following instructions in the command window. "Current date" denotes the new directory name and n is a number, 1 through 6 corresponding to the transducer slot being operated.

```
mkdir ~/tests/current date  
cd ~/tests/current date  
aal/calibtran -t n
```

This starts the program to give a prompt. The frequency in KHz and the gain value are entered:

```
freq 22.18  
gain 2500
```

Typical gain values are from 3100 to 1500, with larger output voltages at smaller gain values. The frequency value should be close to the resonant frequency of the transducer.

Next the measurements are entered. The operator types in the V, I, and phase data from the scope. Phase is taken as the difference "Delta" in time between crossing points for the current and voltage waveforms. With the return command, the system automatically records these values along with simultaneous measurements of the computer-based measurements on the given line of data. Five or six sets of data are obtained at voltages ranging from approximately 20 to 150 volts. The data entry, for example if the delta is 2.0, the voltage is 12.5 and the current is 160 will be:

s 2.0 12.5 160

The gain is changed between each set of data to obtain voltage, current, and phase data as a function of the total acoustic power.

The experiment is repeated for each transducer, beginning with the aal/calibtran -t n instruction. The final instruction:

Quit

saves the log file for off-line analysis.

Typical results from such an experiment are shown in Table 5. The meanings of the column headings are added after the table. In acquiring the data shown in the table, two entries were made for each set of measurements. The first entry contains no scope measurements (1 1 1) was entered) and was obtained at the same time that the scope recording was paused to retain the current values. The second entry has these values, and typically slightly different results for the computer measurements. The data were analyzed by comparing the computer measurements from the first sets of data with the scope measurements in the second sets. This insured that both sets were obtained simultaneously to eliminate the effect of any changes with time as the transducers warmed-up.

With these data, calibration constants are generated to convert computer-measured voltage, current, and phase values into actual voltage current and V-I phase differences and the relation between gain and amplifier voltage. The data are recorded at

~/tests/current date

In Table 5.1, Delta is the displacement of the current and voltage waveforms in units of microseconds. PkI is the peak-to-peak voltage in mv across a 1 ohm resistor. PkV is the voltage measured with a 10X probe, i.e., 1/10 of the actual peak-to-peak value of the voltage waveform. The computer measurement of the current-voltage phase difference is determined by the values of PhiV and PhiI, as discussed later in the section on calibrations.

Table 5 Calibration of transducer electrical characteristics*

Now	Bid	Gain	Freq	Vo	PhiV	Io	PhiI	Delta	PkV	PkI
1299777557	t1	3000	222000	672	3140	345	0	1	1	1
1299777643	t1	3000	222000	672	3147	348	0	-1.1	3.12	117
1299777683	t1	2600	222000	1235	3157	628	0	1	1	1
1299777725	t1	2600	222000	1236	3143	620	0	-.9	5.92	228
1299777760	t1	2200	222000	1803	3120	882	0	1	1	1
1299777774	t1	2200	222000	1804	3111	873	0	-1.1	8.88	328
1299777799	t1	1800	222000	2368	3067	1114	0	1	1	1
1299777824	t1	1800	222000	2366	3035	1074	0	-1.5	11.68	408
1299777866	t1	1200	222000	3213	2975	1362	0	1	1	1
1299777928	t1	1600	222000	2649	2918	1014	0	1	1	1
1299777945	t1	1600	222000	2651	2916	1010	0	-2.4	13.4	376
1299777964	t1	2000	222000	2085	2921	797	0	1	1	1
1299777978	t1	2000	222000	2084	2926	804	0	-2.5	10.24	288
1299778005	t1	2500	222000	1377	2937	547	0	1	1	1
1299778020	t1	2500	222000	1377	2948	553	0	-2.3	6.72	196
1299778070	t1	2700	222000	1094	2971	458	0	1	1	1
1299778083	t1	2700	222000	1095	2977	463	0	-2.1	5.28	159
1299778098	t1	3000	222000	672	2969	296	0	1	1	1
1299778121	t1	3000	222000	673	2983	300	0	-1.9	3.16	97.6
1299778146	t1	3200	222000	379	2957	186	0	1	1	1
1299778164	t1	3200	222000	391	2968	189	0	-1.8	1.72	54.8
Time, sec	board ID		0.1 Hz units	value computer	phase V	value computer	phase I	phase scope	volts	mamp

* Calibration scan (Thu Mar 10 11:10:47 CST 2011)

5.9.3 Resonant Frequency Calibration

The purpose of these experiments is to obtain a set of data that yields the relation between the I-V phase difference and the difference between the operating frequency, F, and the resonant frequency, FR, of a transducer. Table 6 presents the results of a typical experiment. In this experiment, the voltage output of the transducer was held constant and the operating frequency varied from 22,200 Hz to 22,150 Hz and back, in 2 Hz increments. The experiment was performed quickly such that, even though the resonant frequency may drift slightly during the experiment, the average resonant frequency for the two measurements at each frequency was nominally constant.

With the calibrations of section 5.9.2, one obtains plots of the electrical power vs frequency. The plots are symmetrical with a maximum at the resonant frequency. The derived value of FR allows the relationship between F – FR and the I-V phase difference to be derived. This relationship is then used in levitation experiments to follow the value of FR by measuring the I-V phase difference.

The program to perform the resonant frequency calibration is started by the following operations entered in the Inferno command shell:

```
mkdir ~/tests/current date
cd ~/tests/current date
```

```

aal/scanfreq -g 2500 -l 22.13 -h 22.24 -m 500 > g2500.txt
aal/scanfreq -g 2000 -l 22.13 -h 22.24 -m 500 > g2000.txt
aal/scanfreq -g 1500 -l 22.13 -h 22.24 -m 500 > g1500.txt

```

This produces three frequency scans at fixed gains of 2500, 2000, 1500 in the example over the range in KHz defined by low to high, here 22.13 to 22.24 KHz with a 500 ms delay between measurements. The frequency interval for each measurement is 2 Hz. The scan starts high goes low and back to high so that the average resonant frequency for the two measurements at each operating frequency is nominally constant even if the resonant frequency drifts slightly during the experiment.

The data are in the created directory and files for all six transducers. They are analyzed off-line to derive the relationship between resonant, operating frequencies and the I-V phase difference. The results in Table 6 show only the data for transducer t2.

Table 6 Resonant frequency calibration data

N	ID	Gain	10F, Hz	Vo	PhiV	Io	PhiI
0	t2	1500	222000	2840	2921	1613	0
1	t2	1500	221980	2840	2983	1733	0
2	t2	1500	221960	2843	3053	1854	0
3	t2	1500	221940	2841	3125	1978	0
4	t2	1500	221920	2842	3205	2096	0
5	t2	1500	221900	2842	3296	2203	0
6	t2	1500	221880	2843	0	2294	3248
7	t2	1500	221860	2843	0	2375	3151
8	t2	1500	221840	2835	0	2428	3050
9	t2	1500	221820	2844	0	2455	2948
10	t2	1500	221800	2846	0	2455	2852
11	t2	1500	221780	2846	0	2440	2760
12	t2	1500	221760	2847	0	2400	2673
13	t2	1500	221740	2847	0	2350	2592
14	t2	1500	221720	2847	0	2288	2515
15	t2	1500	221700	2848	0	2224	2449
16	t2	1500	221680	2847	0	2153	2391
17	t2	1500	221660	2847	0	2087	2335
18	t2	1500	221640	2848	0	2019	2287
19	t2	1500	221620	2848	0	1958	2246
20	t2	1500	221600	2848	0	1896	2202
21	t2	1500	221580	2847	0	1838	2169
22	t2	1500	221560	2847	0	1784	2138
23	t2	1500	221540	2848	0	1734	2109
24	t2	1500	221520	2848	0	1685	2083
25	t2	1500	221500	2848	0	1638	2058
26	t2	1500	221500	2848	0	1639	2059
27	t2	1500	221520	2847	0	1686	2085
28	t2	1500	221540	2847	0	1735	2111

Table 6 Resonant frequency calibration data, continued

N	ID	Gain	10F, Hz	Vo	PhiV	Io	PhiI
29	t2	1500	221560	2847	0	1786	2141
30	t2	1500	221580	2848	0	1842	2175
31	t2	1500	221600	2848	0	1900	2214
32	t2	1500	221620	2848	0	1962	2253
33	t2	1500	221640	2847	0	2027	2297
34	t2	1500	221660	2847	0	2093	2350
35	t2	1500	221680	2848	0	2162	2407
36	t2	1500	221700	2846	0	2229	2470
37	t2	1500	221720	2847	0	2299	2540
38	t2	1500	221740	2846	0	2357	2621
39	t2	1500	221760	2846	0	2407	2705
40	t2	1500	221780	2846	0	2445	2800
41	t2	1500	221800	2844	0	2460	2900
42	t2	1500	221820	2844	0	2446	3004
43	t2	1500	221840	2844	0	2405	3110
44	t2	1500	221860	2843	0	2344	3217
45	t2	1500	221880	2843	2272	2252	1035
46	t2	1500	221900	2835	3218	2142	0
47	t2	1500	221920	2841	3132	2023	0
48	t2	1500	221940	2841	3052	1898	0
49	t2	1500	221960	2841	2978	1765	0
50	t2	1500	221980	2840	2909	1639	0
51	t2	1500	222000	2842	2851	1520	0

5.9.4 Exactus Pyrometer Data

If “Start” is selected at the bottom of the Exactus pyrometer screen on the GUI, pyrometer measurements are acquired and stored at the selected rate until the operator selects “Stop”. The data are recorded in a file at:

~/logs/exactus/(file name automatically = initial date and time of the experiment).

The file name is shown at the bottom of the Exactus pyrometer screen. After the experiments is completed, the data in this file can be read directly into the Exactus software program, in the Windows operating system or transferred to another computer and examined with the Exactus software.

Each time the user clicks the 'X' or 'Y' scan button, the output is placed in the same directory as the Exactus data file (\$home/logs/aal/exactus). It will have a file name that includes date, time, and “scanX” or “scanY”.

The X and Y scans are logged whether or not the “Start” button has been selected to record pyrometer data.

An example of the X and Y file contents is given below:

```
# AAL/Pyro Scan Y 1312567709 Fri Aug 05 13:08:29 CDT 2011
6.500 5.250 580
6.500 5.275 563
6.500 5.300 584
...
```

The columns are:

```
1 - X mm
2 - Y mm
3 - Exactus temperature
```

The user may click on the temperature line of an X or Y scan to reposition the pyrometer. When this is done, the X and Y position parameters indicated on the screen will change, however the new pyrometer X, Y values are not recorded. A second X or Y scan should be performed to record the new values.

5.9.5 Sensor Data Acquisition

If the “Log” boxes are checked on the sensor screen of the GUI, a file of data is created that records the instructions from the sensors to the acoustic controller. This file contains a continuous record of the data that are shown on the sensor screen, i.e., 250 values per second of the phase change instructions sent to the acoustic controller and the GUI. The record is at:

~/logs/sensor/(file name automatically = initial date and time of the experiment).

5.9.6 AAL Operating Parameters

The parameters shown on the AAL console are automatically recorded in every experiment. The record is at:

~/logs/console/(file name = initial date and time of the experiment).

Table 7 shows part of a typical record. Each group of six lines shows the properties measured from the acoustic boards identified as Bid 1 to 6, i.e., for transducers XA, XB, YA, YB, ZA, ZB respectively. Entries occur every 10 seconds, although updating of the acoustic controller frequency is every 2 seconds and voltage values every 5 seconds when frequency and SPL tracking are turned on. The 0's in the headers indicate that tracking is off. The records that follow were obtained later, after tracking was turned on.

The selected SPL value was increased from 0.8 to 1.0 between the second and third set of measurements in the table. An extra line of data records this event. The numbers following the new SPL value in this line are the old and new gain values required to effect the change in acoustic output.

Table 7 AAL operating parameters.

AAL Console started Mon May 02 13:56:20 CDT 2011
 1304362580 Track SPL: 0
 1304362580 Track Resonant Frequency: 0

Time	Bid	Gain	Freq	Phase	M	Mfreq	Vo	PhiV	Io	PhiI	fan	Vi	Ii	Phic	Phi	p	SPL	Vc	FR
1304362703	t1	2034	22.1501	159	0	0.0000	2043	0	1392	3211	1	10.080	506.827	6.480	6.480	50.76	0.807	2036.56	22.1459
1304362703	t2	1840	22.1501	2048	0	0.0000	2362	3256	1884	0	1	11.536	680.124	-4.048	-4.048	78.26	0.804	2370.09	22.1414
1304362703	t3	2098	22.1501	159	0	0.0000	2051	0	1493	3011	1	10.054	541.511	17.288	17.288	51.98	0.802	2050.50	22.1502
1304362703	t4	2059	22.1501	2048	0	0.0000	2042	0	1450	3273	1	9.922	527.365	3.129	3.129	52.25	0.810	2036.63	22.1453
1304362703	t5	2150	22.1501	159	0	0.0000	1953	0	1655	2704	0	9.726	602.585	33.878	33.878	48.66	0.791	1945.95	22.1594
1304362703	t6	2146	22.1501	2048	0	0.0000	1916	0	1617	2635	0	9.342	583.899	37.607	37.607	43.22	0.789	1911.46	22.1604
1304362713	t1	2031	22.1503	159	0	0.0000	2020	0	1388	3220	1	9.967	505.371	5.992	5.992	50.09	0.801	2040.80	22.1459
1304362713	t2	1847	22.1503	2048	0	0.0000	2353	3241	1881	0	1	11.492	679.041	-4.857	-4.857	77.76	0.802	2360.21	22.1412
1304362713	t3	2103	22.1503	159	0	0.0000	2045	0	1493	3033	1	10.025	541.511	16.097	16.097	52.16	0.803	2043.45	22.1498
1304362713	t4	2066	22.1503	2048	0	0.0000	2032	0	1437	3281	1	9.873	522.637	2.696	2.696	51.55	0.804	2026.77	22.1453
1304362713	t5	2147	22.1503	159	0	0.0000	1958	0	1670	2704	0	9.751	608.047	33.876	33.876	49.22	0.795	1950.18	22.1596
1304362713	t6	2140	22.1503	2048	0	0.0000	1931	0	1623	2657	0	9.416	586.065	36.416	36.416	44.41	0.800	1919.97	22.1601
1304362720	Set	SPL: 1((t1: (2046,1695)),(t2:(1849,1436)),(t3:(2106,1747)),(t4:(2066,1704)),(t5:(2142,1801)),(t6:(2128, 1735)),)																	
1304362723	t1	1695	22.1500	159	0	0.0000	2523	0	1758	3217	1	12.448	640.088	6.156	6.156	79.22	1.008	2516.58	22.1457
1304362723	t2	1436	22.1500	2048	0	0.0000	2924	3248	2364	0	1	14.281	853.404	-4.481	-4.481	121.50	1.002	2940.46	22.1411
1304362723	t3	1753	22.1500	159	0	0.0000	2538	0	1872	3031	1	12.441	678.974	16.208	16.208	81.12	1.002	2537.02	22.1496
1304362723	t4	1697	22.1500	2048	0	0.0000	2550	0	1785	3308	1	12.390	649.205	1.239	1.239	80.42	1.005	2546.91	22.1444
1304362723	t5	1804	22.1500	159	0	0.0000	2442	0	2086	2712	0	12.161	759.513	33.446	33.446	77.07	0.995	2434.39	22.1591
1304362723	T6	1800	22.1500	2048	0	0.0000	2409	0	2038	2615	0	11.746	735.922	38.688	38.688	67.47	0.986	2402.36	22.1608
1304362733	T1	1693	22.1495	159	0	0.0000	2526	0	1752	3218	1	12.463	637.903	6.106	6.106	79.05	1.006	2519.41	22.1451
1304362733	T2	1438	22.1495	2048	0	0.0000	2927	3229	2354	0	1	14.295	849.794	-5.512	-5.512	120.92	1.000	2937.63	22.1401
1304362733	t3	1753	22.1495	159	0	0.0000	2540	0	1874	3026	1	12.451	679.700	16.482	16.482	81.15	1.002	2537.02	22.1492
1304362733	t4	1697	22.1495	2048	0	0.0000	2550	0	1787	3312	1	12.390	649.932	1.027	1.027	80.52	1.005	2546.91	22.1438
1304362733	t5	1799	22.1495	159	0	0.0000	2450	0	2087	2706	0	12.201	759.877	33.774	33.774	77.07	0.995	2441.45	22.1588
1304362733	t6	1793	22.1495	2048	0	0.0000	2422	0	2053	2639	0	11.810	741.338	37.394	37.394	69.56	1.001	2412.29	22.1598
1304362743	t1	1685	22.1491	159	0	0.0000	2538	0	1748	3217	1	12.522	636.447	6.163	6.163	79.24	1.008	2530.74	22.1448
1304362743	t2	1427	22.1491	2048	0	0.0000	2943	3204	2350	0	1	14.374	848.350	-6.866	-6.866	121.06	1.000	2953.16	22.1391
1304362743	t3	1744	22.1491	159	0	0.0000	2552	0	1871	3020	1	12.510	678.612	16.809	16.809	81.27	1.003	2549.71	22.1490
1304362743	t4	1701	22.1491	2048	0	0.0000	2545	0	1789	3309	1	12.366	650.659	1.192	1.192	80.44	1.005	2541.27	22.1434
1304362743	t5	1784	22.1491	159	0	0.0000	2471	0	2106	2710	0	12.306	766.795	33.560	33.560	78.63	1.005	2462.63	22.1583
1304362743	t6	1797	22.1491	2048	0	0.0000	2412	0	2043	2628	0	11.761	737.727	37.991	37.991	68.38	0.993	2406.62	22.1596

With frequency tracking on, the acoustic frequency is set to the average resonant frequency after each set of measurements, every 2 seconds. With SPL tracking on, new gain values maintain the specified SPL value every 5 seconds. Current and I-V phase difference in each circuit vary as the resonant frequency drifts with temperature. The gain values change to keep the power constant by changing the acoustic output voltages.

5.9.7 Entry of Calibration Constants

The following files are text files that contain the calibration data.

~/lib/transducer.cfg

~/lib/sensor.cfg

~/lib/pyro.cfg

The transducer file is changed using a text editor to raise, change and save the file. One can use the editor: acme on the Inferno task bar or the editor: gedit in the Linux applications menu.

The sensor and pyrometer files are edited in the GUI application. One simply changes the values in the GUI and the system retains the new calibration data for future experiments. The existing files are overwritten, so it would be wise to maintain a notebook with values used over time.

The contents of each of these files is illustrated below.

Transducer:

```
(date "Mon Mar 21 16:34:02 CDT 2011")
(IVPc "7.378E+07")
(t1 (sn "12") (tsn "10A") (Av "0.004934") (Ai"0.3641")
    (Aspl "0.11320") (Ag "-1.4160") (Bg "4916.7")
    (A1 "0.4526") (A0 "-7.121"))
(t2 (sn "14") (tsn "1B") (Av "0.004884") (Ai "0.3610")
    (Aspl "0.09092") (Ag "-1.4118") (Bg "4967.8")
    (A1 "0.4754") (A0 "-6.760"))
(t3 (sn "18") (tsn "2A") (Av "0.004902") (Ai "0.3627")
    (Aspl "0.11121") (Ag "-1.4102") (Bg "5009.1")
    (A1 "0.5050") (A0 "-8.613"))
(t4 (sn "16") (tsn "3A") (Av "0.004859") (Ai "0.3637")
    (Aspl "0.11202") (Ag "-1.4096") (Bg "4939.0")
    (A1 "0.4615") (A0 "-6.213"))
(t5 (sn "17") (tsn "2B") (Av "0.004980") (Ai "0.3641")
    (Aspl "0.11335") (Ag "-1.4117") (Bg "4981.1")
    (A1 "0.4603") (A0 "-6.255"))
(t6 (sn "15") (tsn "X3") (Av "0.004876") (Ai "0.3611")
    (Aspl "0.12008") (Ag "-1.4188") (Bg "4956.2"))
```

(A1 "0.4334") (A0 "-5.949")
(SpinMultiplier "2.1")
(SpinOffset "-8.0")

Sensor:

(date"TueMar2917:15:17CDT2011")
(X (sensitivity ".00234562"))
(Y (sensitivity ".00231741"))
(Z (sensitivity ".00200134"))

Pyrometer:

(date"FriApr2917:18:38CDT2011")
(x "37479")
(y "37125")
(swidth "4.5")
(sheight "4.5")

5.9.8 Programming the Acoustic and Sensor Circuits

The programmer's manual addresses the issue of programming chips on the acoustics and sensor electronic circuit boards. These circuits contain dsPIC chips that are programmed using a Microchip PIC programmer device. Further information is available at

<http://www.microchip.com>

The acoustic control boards also have XILINX CPLD chips that are programmed with a XILINX Model DLC10 Platform Cable USBII device. Further information is available at:

<http://www.xilinx.com>

The boards are pre-programmed to operate the AAL. If needed, replacement boards would also be programmed and operate correctly when inserted into the controller or replace boards in the sensor circuit.

5.9.9 Laser Power Log

The aal/uc2k program creates a new log file in \$home/logs/aal/uc2k every time it is started. The output format can be parsed with common tools such as awk, perl, or standard shell scripts. The laser power files are the only files contained in the given directory. They are named with the creation date and time. An example laser power log file is given below.

```
1312489379 UC2K Started: Thu Aug 4 15:22:59 CDT 2011  
1312489400 CONNECT synradone
```

```

1312489400 STATUS synradone mode: %s control: %d pwmfreq: '%s' onup: %d
    maxpwm: %d gate: %d power: %d lase: %d pwm: %.1f
1312489402 CONNECT synradtwo
1312489402 STATUS synradtwo mode: %s control: %d pwmfreq: '%s' onup: %d
    maxpwm: %d gate: %d power: %d lase: %d pwm: %.1f
1312489420 SETPWM synradone 5.0
1312489420 SETPWM synradtwo 5.0
1312489421 LASE synradone ON 5.0
1312489421 LASE synradtwo ON 5.0
1312489425 SETPWM synradone 5.5
1312489425 SETPWM synradtwo 5.5
1312489435 SETPWM synradone 10.0
1312489435 SETPWM synradtwo 10.0
1312489440 LASE synradone OFF 10.0
1312489440 LASE synradtwo OFF 10.0
1312489445 SETPWM synradone 0.0
1312489445 SETPWM synradtwo 0.0
1312489432 SHUTDOWN synradone
1312489432 SHUTDOWN synradtwo

```

5.9.10 Software Extensions

Operating experience with the AAL has revealed some extensions to the AAL software that will become available in the future. These include:

1. Modify pyrometer logging software to add interactive gnu plot for the full temperature data stream.

6. Utility Requirements

6.1 CO₂ Laser Cooling

Synrad recommends that separate closed cycle coolant chillers be used for each CO₂ laser and the associated laser power supplies. Each coolant chiller should have a cooling capacity of 6,000 watts and a water flow rate up to 4 gallons per minute at a pressure of less than 70 psig (15.1 liters/minute at less than 480 KPa). The coolant temperature must be set above the ambient dew point, to avoid condensation of moisture on the power supplies and lasers. Full details are in the Synrad Evolution Operator's Manual at <http://www.synrad.com/evolution/evo240.htm>. Tap water cooling can be used with care if the ambient humidity is low.

6.2 Electrical Power

Two single phase, 240 volt 30 amp electrical power circuits are required. One circuit supplies power for the AAL electronics equipment and associated instruments. The second circuit supplies the three acoustic power supplies.

Four three phase or single phase 240 volt 30 amp power circuits are required for the heating lasers. Two separate sets of power supplies are used for each of the two CO₂ heating lasers.

Wall-plug power is used for the video monitor and the computer.


6.3 Levitation Gas


Levitation gas at flow rates up to the flow controller capacity, currently 5 liters/minute. With addition of ring nozzle flow to limit air oxidation of samples levitated in argon gas, an additional flow of up to 10 liters/minute would be required.

7. Levitation and Materials Processing

7.1. Start-up

The steps given below are followed in start-up of levitation and material processing experiments.

1. The gas jet is adjusted to be nearly vertical. This is done by inserting a long steel rod, of 0.09" = 2.3 mm diameter, into the ceramic tube that supplies the gas. A plumb line is used to check if the rod is vertical. Best control of levitation has been observed if the gas jet is slightly inclined, by 0.10 degree towards the Vision Research camera. This occurs if the steel rod is approximately ½ of its diameter from plumb in 24" = 60 cm.
2. Start-up – allow approximately 30 minutes for the system to warm up after the following operations are completed:
 - Remove lens covers from the pyrometer and the Infinity long distance microscope lens on the Vision Research camera.
 - Turn on the key-switch of the acoustic controller, the acoustic power supplies, the power control panel, and power to the system instruments.
 - Turn on CO₂ laser power supplies and cooling water flow. Check that the water flow valve on the hearth-melter is closed.
 - Turn on gas flow at a small flow rate and power to the gas jet heater. Heater power will be approximately 80% to obtain a gas heater temperature of 500°C.
 - Turn on the GUI and enter the computer password.
 - Click on the following icon. This opens the AAL console, sensor, laser control, and pyrometer screens. 
 - Set the SPL to a value from 0.8 to 1.0 for warm-up and turn on transducer frequency and SPL tracking. The resonant frequencies of the transducers initially differ by about 30 Hz. They trend towards the same frequency as the transducers warm-up.
 - Turn on sensor feedback on the AAL console and sensors screens. Set feedback gain, typically in the range from 5000 to 7500. Click “connected” on the sensor screen.
3. When the gas heater temperature approaches 500°C, increase the gas flow rate to the nominal value required to levitate the sample of interest. Adjust heater control to keep heater temperature below 550°C.
4. Insert the sample to be levitated using the vacuum chuck. Release the sample when it is centered in the marked positions on the two video camera monitors. The gas flow rate must be within a few percent of the required value.

5. Heat the levitated samples with the CO₂ lasers.
 - If sample has an irregular shape, laser beam heating may be required immediately upon sample insertion to achieve successful levitation.
 - The sample is typically heated to incandescence so that the Vision Research camera can be operated at a high frame rate to observe sample rotation. This typically requires 5 to 8% setting for the laser output.
 - Check pyrometer alignment on the levitated sample. With pyrometer centered on the sample, observe the pyrometer output and adjust mirror-mounts for CO₂ beam delivery to maximize sample temperature.
6. Start-up the Vision Research camera. Click the following icon. This raises the VMWare screen. Drag the screen to the second monitor and click the green arrow on the left column of the screen to start or resume Windows XP for operating the Vision Research software. The Phantom camera software is initiated by clicking its icon on the desk top or the start menu.
 

7. Adjust transducer phasing to minimize sample rotation.
 - Rotation was minimized if the spin setting on the AAL console was adjusted according to the equation

$$Spin(^{\circ}) = 2.1(F - F_{AB}) - 8 \quad (7.1)$$

- Here, F and F_{AB} (in Hz) are the operating acoustic frequency and the average resonant frequency of the two transducers for each axis.
 - The spin control parameters are programmed into \$home/lib/transducer.cfg and may be changed if the operators determine an improved spin control function. The values obtained from the programmed function are displayed on the AAL Console screen on the right side of the spin entry field for each axis. The left side of the field has the values entered by the operator. The operator entries are automatically set to the calculated values by clicking on the spin button at the lower left area of the screen, or individually for each axis by clicking the axis spin button.
 - Sample rotation is monitored with the Vision Research camera and the Spin controls may be further adjusted to reduce spin.
 - If the top of a levitated sample rotates towards transducer XB, YB, or ZB, i.e., the upper transducer of each axis, the spin is reduced by increasing the spin setting for that axis.
 - Spin settings change the phase values equally for transducers A and B for an acoustic axis.
8. When experience indicates that spin is sufficiently limited to allow melting, the laser power may be increased to melt the sample.
 - Best results for melting a sample are obtained if sample rotation about a horizontal axis is eliminated. Rotation about a vertical axis may remain, typically at a slow rate, less than 10 Hz, and does not interfere with melting operations.

9. The two transducers for each acoustic axis automatically start-up with a 180° phase difference with spin settings equal to 0°. The AAL console shows 0° for transducer A and 180° for transducer B on each acoustic axis. The 180° phase difference places an acoustic node nominally half-way between the two transducers if the sound speed is uniform or symmetrical in the intervening distance. Heating a levitated sample results in a slightly unsymmetrical sound speed and the A-B transducer phase difference is adjusted to maintain the node positions. Typically, the phase of the A-transducer is increased by 14° when the sample is heated to 1500°C. This adjustment yields good stability at sample temperatures up to 2700°C. Transducer positioning adjustments may be required to obtain good stability at higher temperatures and maximum stability at any temperature.

The lower left area of the AAL Console screen has an entry field for Phase A on all three axes. If the cursor is set on the Phase A entry field, up and down arrows change Phase A by $\pm 1^\circ$ and page up or page down keys change Phase A by $\pm 10^\circ$. The arrow keys allow the operator to smoothly increment Phase A while observing stability of the levitated sample. In this way, a value for Phase A may be determined that provides best stability. Typically, levitation stability is reduced if the acoustic node is not centered at the “chessman” position. Stability may be judged by observing the sample image on the fast camera screen or sample velocity variations on the sensor screens.

10. During levitation experiments, the operators:

- Control the gas flow rate during heating and melting to maintain levitation at the marked positions on the viewing screens
- Adjust the neutral density filters on the video cameras to maintain good imaging as the sample temperature increases.
- Set the laser power.
- Update spin settings as resonant frequencies change. (Intense heating of samples has an influence on the transducer temperatures such that all six transducers approach the same resonant frequency.)
- Adjust SPL and feedback gain values to optimize levitation.
- Adjust the phase of transducer A to maintain the acoustic nodes at the levitation position. If the sample is levitated and the acoustic nodes are exactly at the levitation position, the aerodynamic force from the gas flow will exactly balance the sample weight. Then an increase or decrease in the SPL value will not influence to sample position.

7.2 Controls

The following controls are used to levitate and process samples.

1. Gas flow rate. Set at MKS flow controller.
2. Gas heater temperature. Heating turned on/off and temperatures adjusted at power panel.
3. Acoustic intensity, sound pressure level, SPL. Set at Console screen.
4. Spin control parameters. Set at Console screen.
5. Output power of CO₂ lasers for sample heating. Set manually or at Laser power screen.
6. Position sensing feedback gain. Set at Sensor screen.

7. Vacuum chuck. On/off at power panel.
8. Automatic control of acoustic phases to suppress sample oscillation. On/off at the Console screen.

Controls 1-7 are manually set and may be adjusted during the experiment.

Experience in levitation experiments support decisions about the initial controls and adjustments during an experiment, based on:

1. Shape, size, and mass of the specimen.
2. Location of sample images on the video screens.
3. Fast camera images.
4. Position sensor output signals.
5. Temperature measurements with the Exactus pyrometer.

Controls that are typically adjusted by the operators during levitation, heating, melting, and cooling of samples are:

1. Laser power for the two CO₂ lasers.
2. Spin control parameters are adjusted to eliminate sample spin about a horizontal axis and obtain relatively slow sample rotation about a vertical axis before melting is attempted.
3. SPL and position sensing feedback gain may be adjusted.
4. Gas flow rate is manually adjusted to keep the levitated sample image centered at the marked positions on the video screen.
5. Neutral density filters are operated and gain adjustments made on the video cameras.

7.3 Initial Levitation

Levitation is initiated by inserting and releasing a sample using the vacuum chuck, guided by the video cameras. The sample is inserted until it is located at the marked positions on the video monitors, then released and the vacuum chuck is withdrawn. Successful levitation requires that the flow rate be within a few percent of the required value.

Spherical samples are most easily levitated, and may be used to gain experience with the levitator controls and the adjustments needed as samples are laser-beam heated. In a typical experiment, the gas heater temperature is set at 500-550°C. The gas flow rate is adjusted to an estimated value based on the mass of the specimen to be levitated. Once levitation is achieved, the gas flow rate is adjusted to center the video images on the video screen targets.

Samples with an irregular shape are more difficult to levitate because the aerodynamic force varies with sample orientation. Even so, levitation typically occurs for a few seconds before the sample orientation changes. The effect of sample orientation is reduced if the sample is CO₂ laser beam-heated. Therefore, levitation of irregular-shaped samples often requires that the CO₂ laser beam heating be turned on as soon as the sample is released by the vacuum chuck. Heating to approximately 1000°C is usually sufficient to stabilize levitation.

An example of levitation conditions:

- 3.18 mm, 67 mg aluminum oxide sphere
- Nitrogen flow rate = 3100 ± 75 cc(STP)/min.
- Gas heater temperature = 530°C
- Acoustic SPL = 0.9.
- Position feedback gain = 5000.

Gas flow is manually controlled by an experienced operator, via the dial pots at the front of the MKS flow controller. Gas flow rate, F , is usually increased with temperature as a sample is first heated because temperature asymmetry tends to move the acoustic node downward. The gas flow rate then decreases when phase adjustments (via Phase A on the Console screen) restore the acoustic node to the levitation position.

For different materials and sample sizes the gas flow rate is approximately proportional to the square root of sample mass for equal sample diameters and decreases slightly with sample diameter. Changes in flow rate are required when solids melt due to changes in sample shape.

Levitation of spheres results in rapid sample rotation that interferes with melting experiments. The rotation of spheres is difficult to observe and control. A sphere can be carefully heated and cooled to produce partial melting and solidification to change the sample shape. This improves the ability to observe and control sample spin and rotation.

Rotation of levitated samples about a horizontal axis results from slightly non-vertical gas flow and if the acoustic node position is not centered on the gas flow axis. Careful alignment of the acoustics and gas jet, and operation of the spin controls can eliminate horizontal axis rotation. Slow rotation about a vertical axis is then observed. When a sample is melted sample rotation about a horizontal axis is eliminated and the gas flow stirs the melt. Melts continue to rotate about the vertical axis.

7.4 Heating and Melting

CO₂ laser beam heating is controlled from the system computer via the graphical user interface or by manual operation of the laser control panels. The laser control panels have “select” and “enter” panels used to specify the method of laser control. The “select” panel has three options, “RS232” for computer control of the lasers, “Manual” for control via the knobs on the laser control panels, and “analog” which is not implemented in the AAL system. The user presses “enter” with the desired option selected. Manual control is often used for laser hearth melting experiments and computer control for experiments on levitated samples.

Manual control of the gas flow rate is required to maintain levitation at the desired position when a sample is CO₂ laser beam-heated. The flow rate increases with the sample temperature and usually decreases when a sample is first melted. Rapid solidification of a levitated liquid preserves the liquid shape so that rapid cooling, solidification and re-melting can occur with minimal or no change in the gas flow rate.

Two flow control dials are provided for manual control of the flow rate during levitation experiments. The fine control dial is initially set to its mid-range value and start-up levitation obtained by adjusting the coarse control dial to the required flow rate. Subsequent changes in flow rate with the levitated and heated sample are then made with either control dial according to the operator's preference. The coarse control dial has proved sufficient for most operations.

With experience, the operator learns the approximate changes in the flow control dial that compensate for change in the levitation forces with temperature and upon melting, and can make these changes in a timely way to preserve levitation of the sample. Some failures may occur while obtaining this experience. Different materials behave differently, depending on sample size, density, surface tension. Higher density samples generally require larger values for the SPL settings. Example SPL values are 0.8 for Al_2O_3 (density 4 g/cm^3) and 1.2 for HfO_2 (density 9.68 g/cm^3).

Levitation is best preserved during melting if the phase change occurs quickly. The sample is first heated to a temperature near the melting point. Then the heating laser power is increased 30 to 50% to produce rapid melting. A reduction in the laser power may then be required to avoid overheating of the melt, which can cause vaporization losses of more volatile components. Undercooling of liquids under containerless conditions allows the laser heating power to be reduced to less than the initial value and still maintain a completely liquid sample.

The SPL (sound pressure level) of the acoustic levitator may be increased during melting to help compensate for changes in the aerodynamic levitation force with sample shape. After melting is complete the SPL value can be reduced.

A laser kill switch allows the operator to immediately terminate laser heating power. It is connected in a circuit that allows additional laser kill switches for laboratory safety purposes. The switch can be used for off/on operation of the lasers at fixed laser power settings to perform a sequence of rapid cooling, solidification, reheating, and re-melting experiments on a levitated sample.

7.5 Acoustic Modulation

The AAL Console Screen provides a rudimentary ability to modulate the acoustic intensity of any transducer. The modulation level can be set from 0 to 127% of the SPL value, although the modulation level is also limited by the maximum voltage output of the acoustic power supplies. After selecting the modulation level and frequency, the check box for modulation turns the process on and off. Since modulation of each transducer is initiated separately, two transducers will not in general be modulated in-phase. Modulation of the acoustic force is obtained by holding one transducer at constant output and modulating the output of the opposed transducer at levels from less than up to the output of the first transducer.

For viscous materials, acoustic modulation at low frequencies can be used to observe the rate at which a fluid relaxes when the acoustic compression forces are increased or decreased. The modulation capability does not have an established lower limit on frequency, but frequencies as small as 0.001 Hz are possible.

For inviscid materials, higher frequency modulation may be used to investigate the resonant oscillation frequencies of levitated liquids. Typical frequencies are then in the range from several Hz to 200 Hz. Much greater modulation frequencies are not possible with the highly resonant transducers. To estimate an upper limit for modulation frequency, the output of a transducer was measured with a microphone. When the input to the amplifier was turned off, the acoustic output decayed with a time constant of approximately 8 ms. Thus, at modulation rates much greater than 125 Hz, the acoustic output will tend towards a constant value.

The acoustic force on levitated samples is a compression force if the gas flow rate is adjusted to maintain levitation precisely at the acoustic node. Increasing or decreasing the output of one transducer can then squeeze or relax squeezing of a liquid drop in the direction of the acoustic axis. The force arises from the standing wave produced by interference of the acoustic output of opposed transducer pairs. There will be no change in force when the output of one transducer is increased above that of the other.

8. Transducer Calibration

Calibration of each acoustic transducer is performed with equipment as illustrated in Figure 26. A calibrated 1/8" diameter Bruel & Kjaer (B&K) Model 4138 microphone¹ is mounted 7.5 cm = 3 inches from the surface of the transducer and centered on the vertical acoustic axis. It is connected to a frequency meter capable of measuring 22 KHz with a precision of 0.1 Hz and a digital voltmeter that records the microphone output as Sound Pressure Level (SPL). The SPL and frequency are determined by the output of an acoustic amplifier which is in turn controlled by a preamplifier that provides frequency and SPL control. Voltage (V), current (I), and the V-I phase difference are measured with an oscilloscope. The circuit that senses voltage and current also provides power and on/off control to the transducer cooling fan.

The transducer may also be operated by manual control on the Console screen. The calibration operations discussed here, except for SPL vs acoustic power calibration, can be obtained as described in section 5.

Figures 27-29 illustrate transducer calibration results. Figure 27 shows an experiment to determine the resonant frequency via SPL vs frequency measurements. The figure illustrates that the acoustic output is proportional to the square root of the amplifier output power over a substantial range of off-resonant frequencies.

Figure 28 shows how the difference between operating and resonant frequencies of a transducer depends on the I-V phase difference in the amplifier power circuit. In this case, the operating and resonant frequencies are equal if the I-V phase difference is approximately 13°.

Figures 27 and 28 present data obtained at a relatively low transducer output power, i.e., an SPL value of approximately 0.14 (volts) at resonance as measured with the B&K microphone. By operating at such a low output power, the transducers do not heat up during the experiment and

¹ Equipped with ACO Pacific Model PS9200 Acoustical Interface and Model 4012 preamplifier.

the resonant frequency remains constant. Data obtained at increased power output are given in Figure 29, as SPL vs amplifier power output. It is seen that the SPL values are proportional to the square root of the amplifier power output.

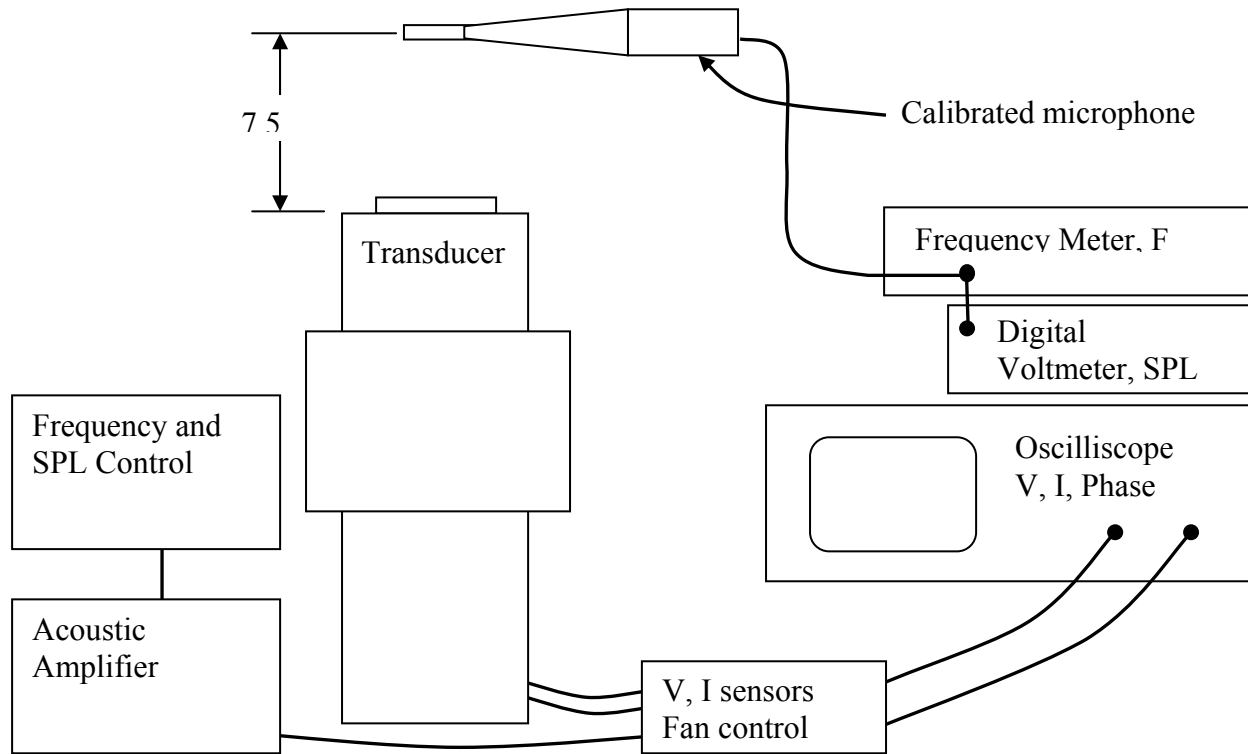


Figure 26 Acoustic transducer calibration facility.

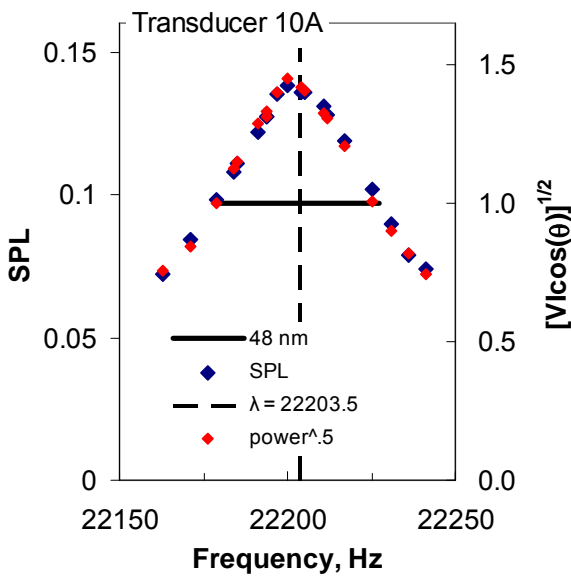


Figure 27 SPL and amp power vs frequency at constant voltage amplifier output.

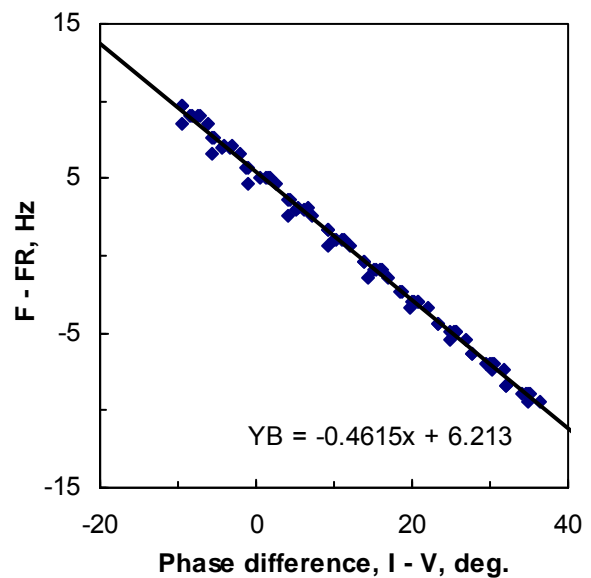


Figure 28 Resonant frequency (FR) minus frequency (F) vs I-V phase difference.

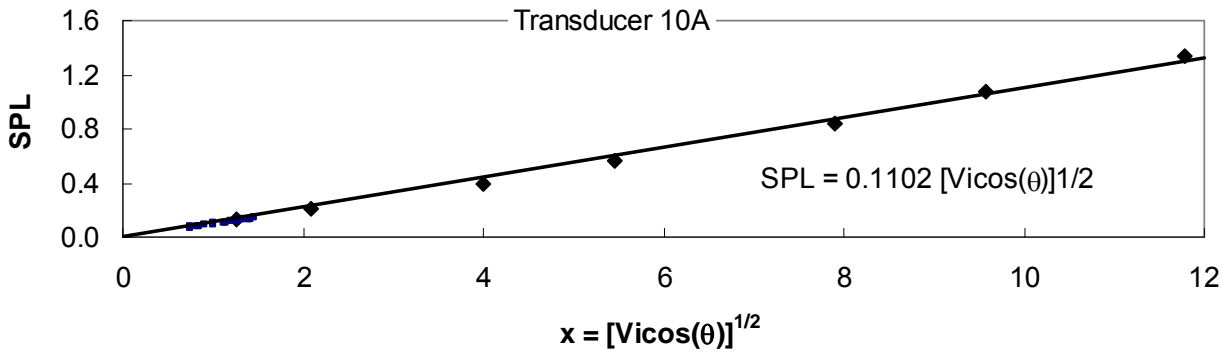


Figure 29 SPL vs amplifier power delivered to the transducer motor.

The results in Figures 27 and 29 show that SPL control is obtained by measuring the amplifier output power, given as the product of V, I, and cosine of the I-V phase difference. The output of the amplifier can thus be controlled to maintain a specified SPL value.

The results in Figure 28 show that the resonant frequency of a transducer can be determined from knowledge of the operating frequency and measurement of the I-V phase difference in the amplifier output.

Additional calibrations are obtained by comparing the voltages, currents, and phases measured with the oscilloscope with the values of these parameters that are measured by the computerized acoustic control system.

The calibration functions for all six transducers are given in the following section on Transducer Algorithms.

9. Transducer Algorithms

In practice the acoustic transducers are computer controlled and monitored by software in the digital circuits installed in the acoustic controller, based on operator instructions provided through the graphical user interface (GUI) on the video monitor. The control parameters are in three different sets, (i) specified by the operator, (ii) measured by the computer, and (iii) calculated from the specified and measured parameters to be used in control of the levitator.

9.1 Operator- and Computer-controlled Parameters

- F, acoustic operating frequency.
- SPL value (acoustic output).
- $\varphi(x)$, $\varphi(y)$, $\varphi(z)$ acoustic phase differences between the two transducers that comprise the 3 orthogonal acoustic axes, the X, Y, Z axes (position control phases).
- $\varphi(xs)$, $\varphi(ys)$, $\varphi(zs)$ acoustic phase adjustments to the three axes for sample spin control
- G_i , the gain values that control the voltage output of the acoustic amplifiers.

With frequency tracking turned on the acoustic frequency, F , is automatically set to the average of the resonant frequencies of the six transducers, which change as the transducers warm up. Computer control also adjusts the output power of each transducer to maintain it at the SPL value selected by the operator. The position control phases are set by the operator. When the position sensing and feedback control system is activated, it adjusts the position control phases to stabilize levitation. The spin control phases are always under operator control, typically set in response to the observation of sample spin before melting of a levitated sample is attempted. The operator can perform experiments with levitated samples that have marks on them to observe sample rotation, and determine spin control parameters that minimize or eliminate the rotation. The gain values, G_i are typically calculated by the computer from automated measurements and used to control amplifier voltages at values that reproduce the operator-selected SPL.

9.2 Computer-Acquired Parameters

Computer-acquired parameters, for the six ($i = 1$ to 6) transducers, in arbitrary units are:

- V_{Ci} , amplifier voltage.
- I_{Ci} , amplifier current.
- $Ph_{Vi} - Ph_{Ii}$, the phase difference between the amplifier output voltage and current.

These properties are acquired by the computer at a frequency of 4 Hz.

9.3 Calculated Parameters

Calculations yield additional parameters from the calibration results applied to the operator-specified and the computer-acquired parameters.

- V_i , the peak-to-peak voltage output of amplifier $i = 1$ to 6.
- I_i , the amplifier current output, as measured as the peak-to-peak voltage across a 1-Ohm resistor.
- Ph_i , the current-voltage phase difference.
- P_i , the amplifier power delivered to each transducer.
- $F_{R,i}$, the resonant frequency of each transducer.
- G_i , gain values that determine the voltage output of each amplifier.

9.4 Voltage, Current, I-V Phase Difference, Amplifier Power

The values of V_i , I_i , Ph_i and P_i are calculated directly from the computerized measurements. The functions used for these calculations are:

$$V_i = A_{Vi} \times V_{Ci} \quad (9-1)$$

$$I_i = A_{Ii} \times I_{Ci} \quad (9-2)$$

$$Ph_{Ci} = \text{Sign}(Ph_{Ii} - Ph_{Vi}) \times \left[1 - \frac{(Ph_{Ii} + Ph_{Vi}) F}{7.378 \times 10^7 \cdot 10} \right] \times 180 \quad (9-3)$$

$$P_i = \frac{V_i \times I_i}{100} \cos(Ph_i) \quad (9-4)$$

The constants in these equations, A_{Vi} and A_{Ii} , are calibration constants given later.

Equation (9-3) is based on the method by which the computerized measurement is obtained. The computer-retained value of the operating frequency, F , is in units of 0.1 Hz, thus, F is divided by 10 in the equation. The phase measurements are obtained by two counters that count cycles of an oscillator operating at a frequency of 7.378×10^7 Hz to obtain Ph_{Ii} and Ph_{Vi} . The counter for I_i is on and the counter for V_i is off for the interval between zero-crossings of the current and voltage signals, if the current signal crosses zero first after the measurement is initiated. Vice-versa if the voltage signal crosses first. Thus, the counting period is at most half an acoustic cycle. The accumulated count is $7.378 \times 10^7 / F$ when the current and voltage are $\pm 180^\circ$ out of phase, and smaller for other phase differences as indicated by the equation. The sign of the phase difference is determined by the counter in which the count accumulates.

The value of P_i obtained from the equations is only proportional to and is not equal to the actual amplifier power because the values of V_i and I_i are peak-to-peak values for the AC signals. The convention of using peak to peak values is consistently used as properties conveniently measured with an oscilloscope. The actual power is not needed by the AAL control algorithms.

9.5 Acoustic Frequency Control

The acoustic frequency, F , is set by the operator on the Console screen. If frequency tracking is selected, the value of F is automatically kept at the average resonant frequency, F_{Ri} , of the six acoustic transducers. The relationship between the operating frequency, the resonant frequency and the I-V phase difference for a transducer is given with sufficient accuracy by the following equation. The calibration coefficients in Equation (9-5), A_{0i} and A_{1i} , are slightly different for each transducer.

$$F_{Ri} - F = A_{1i} Ph_i + A_{0i} \quad (9-5)$$

The transducers are controlled by the following protocol.

1. Use equation (9-5) to calculate the resonant frequency of all transducers from the measured Ph_i values.
2. Average the resonant frequencies.
3. Set F to the average value.
4. If F_{Ri} is greater than F , turn the transducer cooling fan off.

5. If F_{Ri} is less than or equal to F , turn the transducer cooling fan on.
6. Repeat after 5 seconds. The resonant frequencies will decrease as the transducers warm up and increase as they cool down.

On-off control of the transducer fans makes the resonant frequencies drift toward a common value as the transducers warm up. Figure 30 illustrates resonant and operating frequency changes with time during a typical experiment.

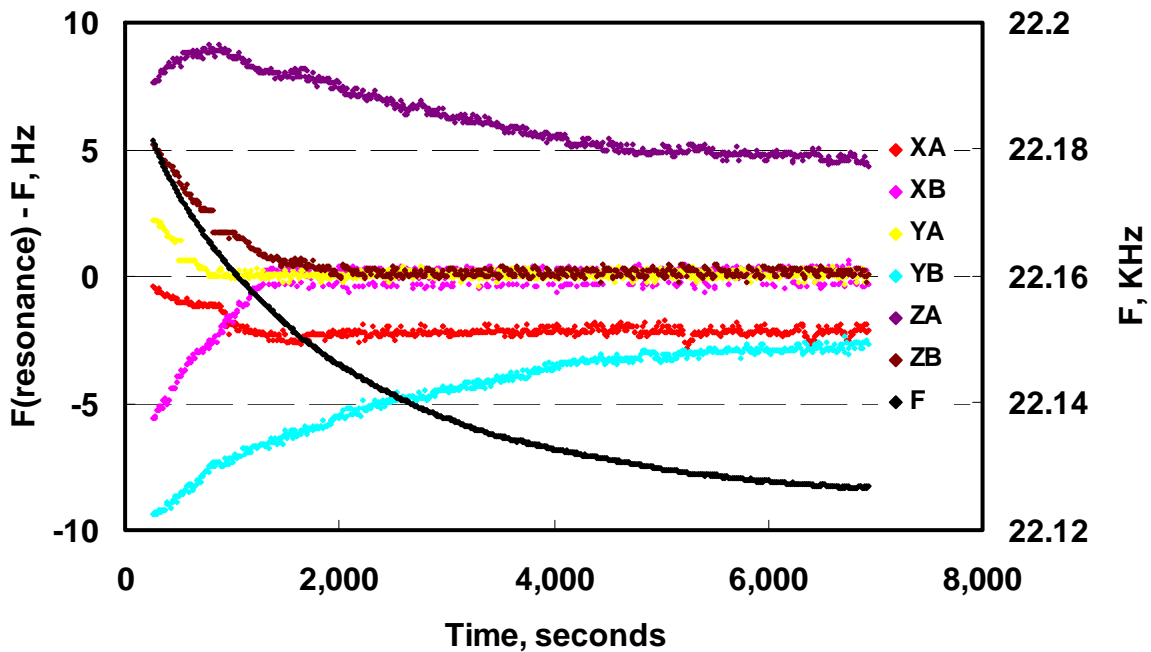


Figure 30 Resonant frequency tracking for a typical experiment, SPL = 0.9.

9.6 Voltage Control to Maintain a Given Value for the SPL

Figure 29 illustrates that SPL is a linear function of the square root of amplifier power, as given by Equation (9-6).

$$SPL_i = A_{SPLi} \times \sqrt{P_i} \quad (9-6)$$

The amplifier output power is controlled by adjusting the gain parameter for the preamplifier signal provided to the amplifier. Voltage output of the amplifier, V_{Ci} as measured in arbitrary units by the computer, is related to the gain parameter, G_i , as given in Equation (9-7).

$$V_{Ci} = A_{Gi} \times G_i + B_{Gi} \quad (9-7)$$

Amplifier output voltages are controlled to maintain the operator-specified SPL value by the following protocol.

1. The operator specifies an SPL value.

2. $P_i(1)$ is calculated for each transducer using Equation (9-6). The P_i values required to achieve the specified SPL will typically differ for all transducers.
3. Measure V_{Ci} , I_{Ci} , Ph_{i1} , Ph_{Vi} .
4. Calculate V_i , I_i , Ph_i and $P_i(2)$ from Equations (9-1) to (9-4).
5. Calculate $V_{2i} \cdot I_{2i}$ equal to the product of V_i and I_i in Equation (9-4) that yields the required power of $P_i(1)$ using the value of Ph_i obtained in step 4.
6. The new voltage values that will yield the specified SPL are then given by

$$V_{2i} = V_i \sqrt{\frac{V_{2i} \times I_{2i}}{V_{Ci} \times I_{Ci}}} \quad \text{and} \quad V_{Ci} = V_{Ci} \sqrt{\frac{V_{2i} \times I_{2i}}{V_{Ci} \times I_{Ci}}} \quad (9-8)$$

7. Use Equation (9-7) to calculate the new value of gain, G_i from the above value of V_{Ci} .
8. Set the gain to the new value.
9. Repeat every 2 seconds.

Calibration constants that appear in the equations of this section are given in table 8.

Table 8 Calibration constants, March 21, 2011.

Board slot		t1	t2	t3	t4	t5	t6
Transducer Board							
Serial Number*		12	14	18	16	17	15
Transducer ID		10A	1B	2A	3A	2B	X3
Transducer position		XA	XB	YA	YB	ZA	ZB
Equations	Parameter						
1	AVi	.004934	0.004884	0.004902	0.004859	0.004980	0.004876
2	Ali	0.3641	0.3610	0.3627	0.3637	0.3641	0.3611
6	ASPLi	0.11320	0.09092	0.11121	0.11202	0.11335	0.12008
7	AGi	-1.4160	-1.4118	-1.4102	-1.4096	-1.4117	-1.4188
7	BGi	4916.7	4967.8	5009.1	4939.0	4981.1	4956.2
9	Ali	0.4526	0.4754	0.5050	0.4615	0.4603	0.4334
9	A0i	-7.121	-6.760	-8.613	-6.213	-6.255	-5.949

10. Transducer alignment

Figure 31 shows the top view of the levitator as if the top plate were transparent. It shows the six transducers for axes X, Y, and Z and the two video cameras, V1 and V2, used for alignment. Each of the three axes has transducer A attached to the bottom plate and transducer B attached to the top plate. The video cameras are shown with an angular separation of 90°, symmetrical about a vertical plane through the X-axis. The video camera mounts can be moved to increase the angular separation to approximately 110° so that the two cameras are nearly in the vertical planes through the Y and Z axes.

Transducer alignment is performed by the following operations. Steps 1-4 are geometric alignment and Steps 5-6 are acoustic alignment.

1. Adjust transducer mounting hardware for each axis so that the geometric axes of transducers A and B are coincident. This may be performed by removing the transducers and adjusting the transducer mounts so that a long 3" diameter tube can be passed through mounts A and B for each axis.

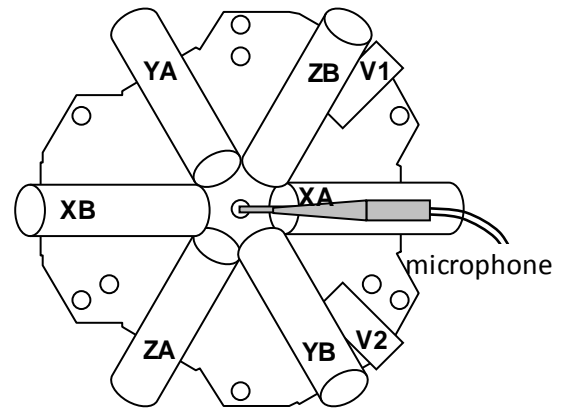


Figure 31 Top view of levitator.

2. Install the centering device “chessman” from the top plate to indicate the aligned position at the center of the levitator structure. The chessman ball should be exactly $9 \frac{7}{8}'' = 25.08 \text{ cm}$ from the surface of its mounting plate. The mounting plate is installed using three $0.375''$ diameter shoulder bolts. An extra hole in the mounting plate and the top plate of the levitator mark the correct orientation of the chessman mounting plate.
3. Adjust the video cameras to be centered on the chessman location and mark that position on the video displays. Then remove the centering chessman. The video cameras are shown with a 90° separation in Figure 31. This angle may be conveniently increased to approximately 110° for alignment purposes, so that cameras V1 and V2 are nearly in the same vertical planes as transducer axes Z and Y, respectively.
4. Install the transducer jig base and transducer chessman on each transducer. Adjust the transducer mounting hardware and the axial position of the transducer to center the chessman on the marked locations of the video displays.

At this point, the transducers are equally distant from the levitation position defined by the chessman. The geometric axes of the transducers pass through the levitation position. Steps 5 and 6 adjust for differences between the acoustic and geometric axes. Steps 7 and 8 adjust for unequal phase differences between the preamplifiers where phases are set and the horn surfaces of each transducer. Some iteration of steps 5-6 steps 7-8 may be necessary.

5. Operate a single acoustic axis with an SPL value of approximately 1.0 and with the A and B transducers exactly 180° out of phase. With uniform temperature, a levitation node will be close to the half-way position between the two transducers. Levitate a small, less than 3 mm Styrofoam ball in the center node. The Styrofoam should be light enough that a further increase in SPL does not influence its axial position. That is, it is light enough that displacement from the node due to gravity is negligible.
6. The object is to achieve the aligned video views of Figure 31. This may require a phase difference other than 180° for the transducer pair and the required phase difference will depend on resonant frequency values of the transducers. No adjustment of the axial position

of the transducers is made during step 6. Adjust the transducer positioning devices, first to obtain vertical alignment with the marked position on the video screens and second to obtain transverse alignment. Figure 32 illustrates typical video observations that may occur during the acoustic alignment process by levitation on each of the three acoustic axes. The vertical displacements should be equal for each camera. The horizontal displacements should be equal for both cameras with X-axis levitation. For Y-axis and Z-axis levitation, horizontal displacements will be larger on the V2 and V1 cameras, respectively. When the transducers are aligned, the levitated Styrofoam ball will pass through the aligned position as the phase difference of the transducer pair is changed.

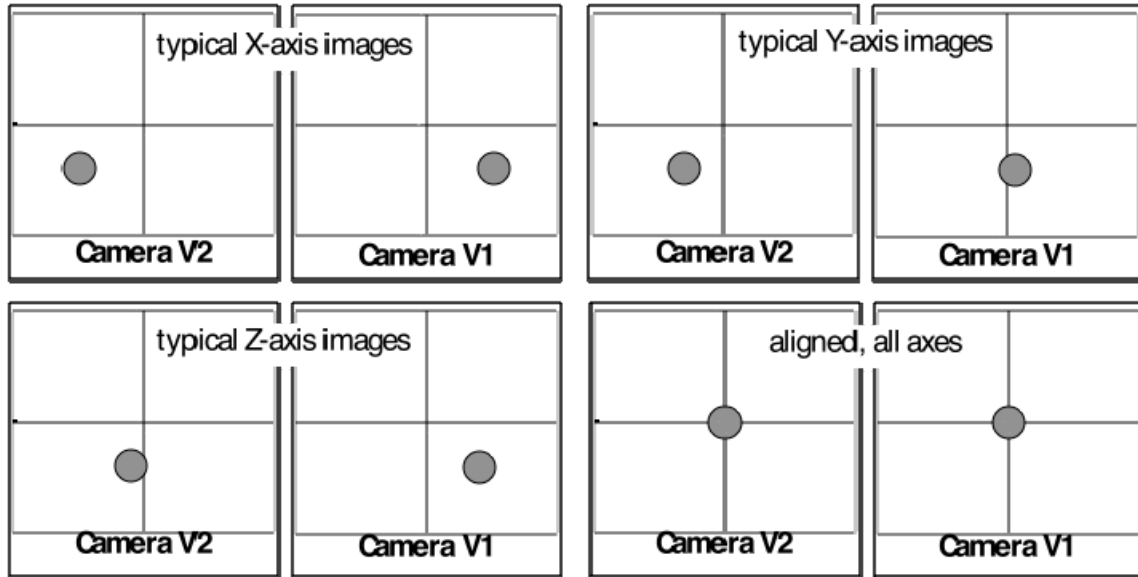


Figure 32 Video camera views of levitated styrofoam during acoustic alignment.

The phase difference between the preamplifier that drives the acoustic power supply and the horn surface varies with the difference between the operating frequency and the transducer's resonant frequency, and can also vary slightly from one transducer to another. The alignment approach used is to adjust the transducer A positions to achieve resonant levitation at the chessman-specified position.

7. Use single axis levitation of Styrofoam at $SPL \approx 1.0$. Set the phase of transducer B at 180° . Measure the phase of transducer A that achieves levitation at the Chessman position, as a function of the resonant frequency difference for the transducer pair. Manual control of the operating frequency and transducer fans allows a range, ca. ± 15 Hz for the resonant frequency differences.
8. Adjust the axial position of transducer A so that levitation occurs at the chessman position when the A-B phase difference is 180° . The typical adjustment is given by Equation 10-1

$$\Delta(\text{transducer}), \text{ cm} = \frac{1.6/2}{360} \times \frac{\text{phase A at resonance}}{\text{from step 6}} \quad (10-1)$$

Equation 10.1 is based on the fact that the wavelength is nominally 1.6 cm in air and the acoustic nodes move a distance equal to half a wavelength if the phase of one transducer changes by 360°.

A plot of the values of Phase A vs resonant frequency difference is given in Figure 33, as obtained after the Equation 10-1 adjustments were completed.

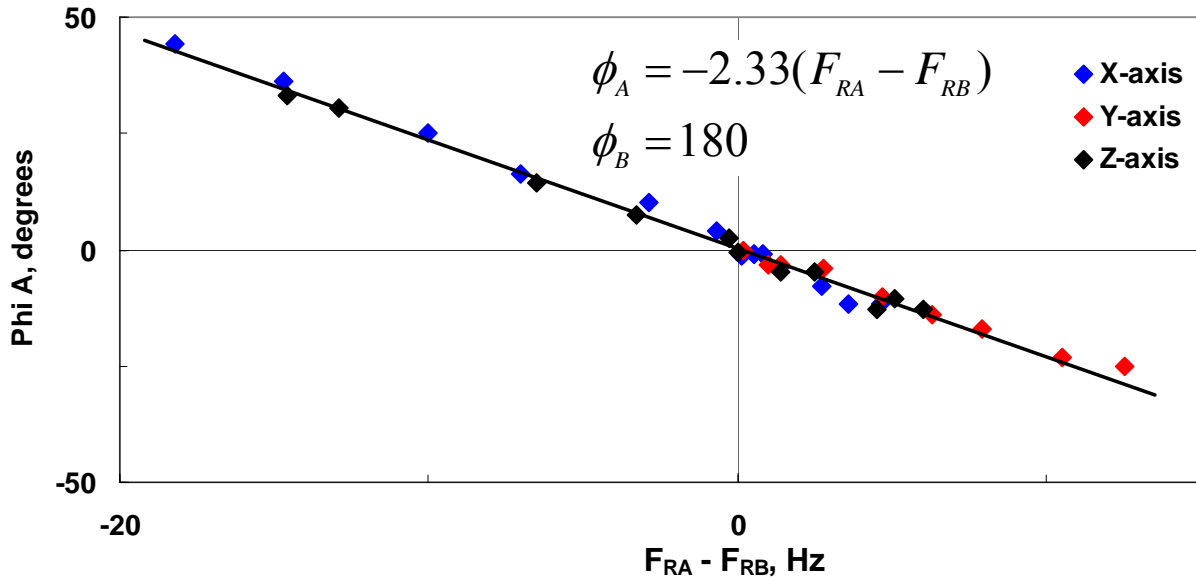


Figure 33 Transducer calibration for off-resonant levitation.

11. Acoustics

Acoustic levitation occurs near nodes in the standing waves created by two opposed transducers operated at equal frequencies. The nodes are at the ambient pressure, in locations where the opposed acoustic waves always cancel. The pressures at anti-nodes oscillate with the standing wave intensity. Positive pressure excursions at the anti-nodes are greater than negative excursions so that the average pressure at an antinode is greater than ambient. Acoustic levitation forces result from the (average) pressure gradient between the nodes and antinodes.

11.1 Reflected Sound Waves

The AAL has three sets of transducers with axes on three orthogonal lines. The transducers are horns that produce most of the sound from their edges. Anti-reflection foam is attached to the centers of the horns to reduce the influence of reflected sound waves on the standing wave pattern. However reflections are not completely eliminated and are estimated to contribute approximately 15% to the acoustic intensities at the levitated position. Reflections may add or subtract from the standing wave pattern, depending on their phase differences with the direct sound waves.

11.2 Sample Oscillation

Disturbances cause the position of a levitated sample to oscillate. For example the shape of a sample changes when it melts and the aerodynamic levitation force changes with the sample shape. Position sensing and feedback control of acoustic forces on a levitated specimen are used to limit the sample motion that disturbances can cause. For this purpose it is useful to understand the frequency at which an acoustically-levitated specimen will oscillate in the acoustic well.

The sample motion is assumed to be harmonic. The frequency, f , at which harmonic oscillation occurs in the acoustic well depends on sample mass, m , and a spring constant, k , which relates displacement to restoring force.

$$f = \frac{1}{2\pi} \sqrt{\frac{k}{m}} \quad (11-1)$$

For a sample levitated by the minimum acoustic forces, the acoustic force on the sample changes by the sample weight in a distance equal to the sample diameter d . In aero-acoustic levitation, the acoustic force is less than the specimen weight. Thus we have, for aero-acoustic levitation:

$$k < \frac{mg}{d} \quad (11-2)$$

$$f < \frac{1}{2\pi} \sqrt{\frac{g}{d}} \quad (11-3)$$

With a typical sample diameter of 0.3 cm and $g = 980 \text{ cm/s}^2$ one obtains $f < 9 \text{ Hz}$.

Some observations on an acoustically levitated styrofoam sample are given in Figure 34. The resonant oscillation frequency was measured as the frequency of on-off operation of one transducer that produced a maximum oscillation amplitude. Smaller amplitudes were seen if the frequency was more than 5% different from the resonant value. The resonant frequency has a linear dependence on the acoustic pressure level. The harmonic spring constant, k is second-order in the sound pressure level.

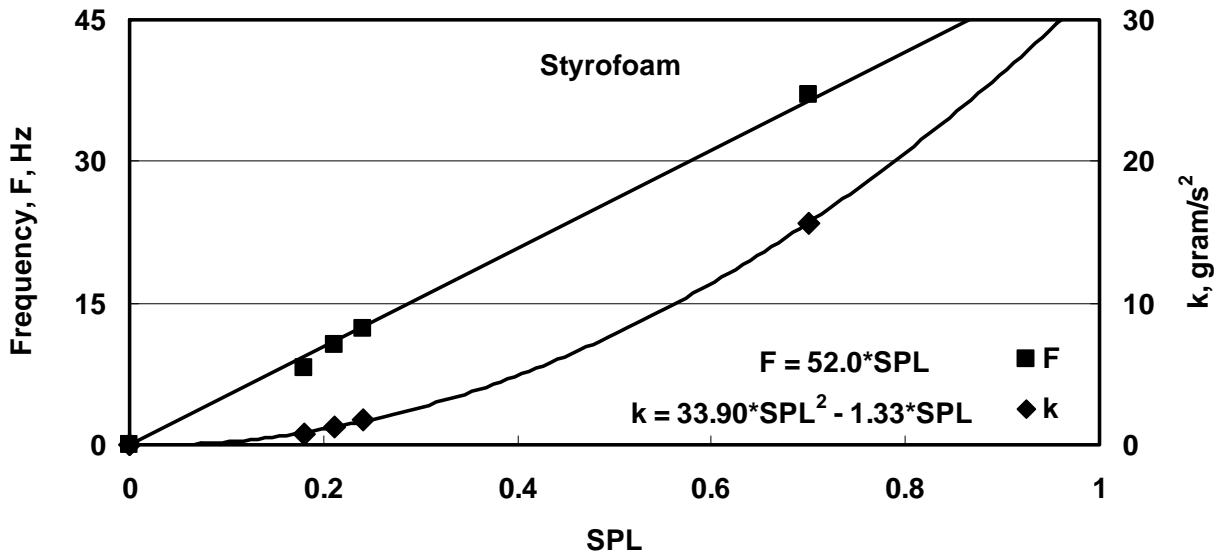


Figure 34 Resonant frequency and spring constant for harmonic vibration of acoustically-levitated Styrofoam.

The Styrofoam sample mass was 0.28 mg and its diameter was 2.6 mm. Levitation failed at SPL values of 0.14 or less. The SPL values required to levitate dense materials could thus be estimated by setting the density ratio with Styrofoam equal to the k-value ratio at SPL = 0.14. The result of this estimate is given in Figure 35. It predicts slightly greater SPL values than are actually required. For example, water drops are levitated at SPL = 0.60, but the results in Figure 35 predict SPL = 0.86 for water. Similar experiments with denser samples would likely give more accurate results.

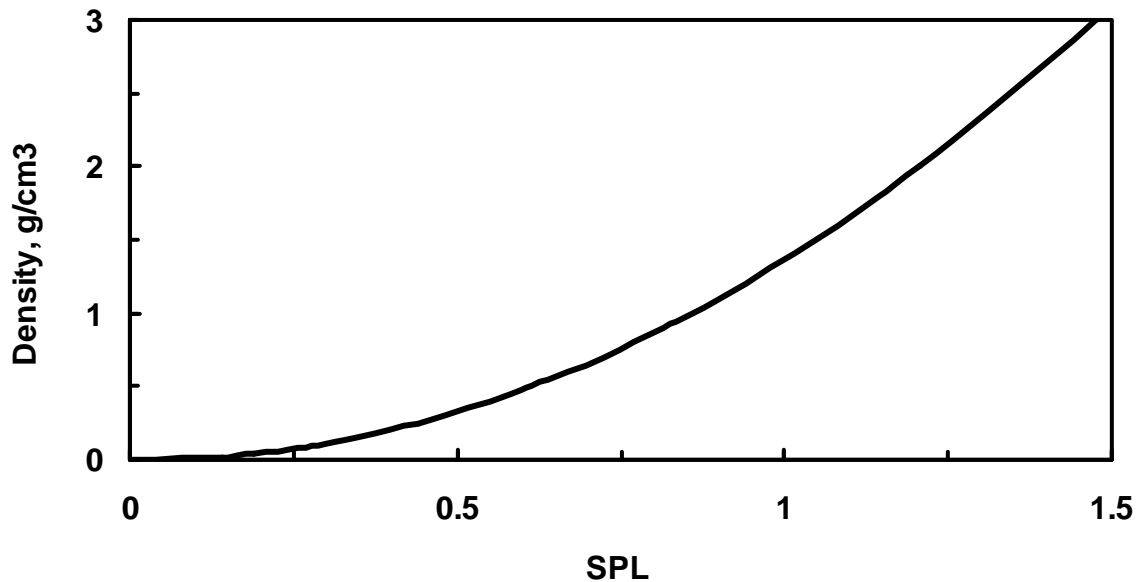


Figure 35 Maximum density for acoustic levitation vs SPL value, estimated from the results of oscillation frequency measurements on a Styrofoam sample.

SPL values should not be increased above 1.5 to minimize wear or damage to the acoustic transducers. Thus it is clear that acoustic levitation alone could not support samples of density greater than about 3 g/cm³. Even then, the acoustic intensity would likely be sufficient to fragment liquid samples.

11.3 Spin Control

An acoustically levitated sample can exhibit spin, depending on the acoustic phase differences at the sample for the three acoustic axes. The phase differences in the preamplifier signals transmitted to the acoustic amplifiers are under operator control via the spin-control settings on the Graphical User Interface (GUI). The phase differences at the acoustic transducers can differ from those in the preamplifier signals if the transducers are operated at off-resonant frequencies. Phase differences at the sample are also influenced by transducer alignment, position of the levitated sample, and reflected acoustic waves.

An acoustic node will occur at the levitation position defined by the chessman if the sound speed is symmetrical in the intervening space and the sound waves are 180° out of phase at the transducer surfaces. An anti-node will be at the half-way point if the transducers are in-phase. Proper alignment has the acoustic axes of all three transducer pairs intersecting at this half-way point. Then, if the transducers are all operated at their resonant frequencies, the upper-three are 180° out of phase with the lower three transducers, and if there are no reflected waves, the sample will not spin. These conditions are never exactly met.

As transducers warm up, their resonant frequencies approach a common value, as described in Section 2.5. Therefore some adjustment of the spin control parameters may be required during the initial warm-up period. Heating of levitated samples also has a small influence on the transducer temperatures, so that spin adjustments after transducer warm-up may also be required.

Section 7.1 discussed protocols to control sample spin by near-vertical alignment of the gas jet and adjusting the spin control values on the acoustic console screen by amounts that depend on the departure of transducers from resonant operation.

11.4 Effect of Sample Heating

The temperature field in the space between two opposed transducers becomes slightly non-symmetrical when a sample is heated and when a levitation gas different than the ambient gas is used. This influences the sound speed and the acoustic phases at the levitated sample relative to the phases at the transducer surfaces. Since all three axes are equally inclined to the vertical, they will exhibit the same nominal departure from symmetry in sound speed. No change in spin control parameters is then required, but changes in the phase difference between upper and lower transducers are made to maintain the acoustic nodes at the desired levitation point. In practice, these changes are not required to achieve levitation for sample temperatures from ambient to more than 3000°C. However, they are required to maximize levitation stability.

For samples of approximately 3 mm diameter, heated to 1500°C, superior stability was found if the Phase A values on the acoustic console screen are increased by 14°. This adjustment yields

good stability at sample temperatures up to 2700°C. A further increase in the phase of transducer A is required to maintain good stability at temperatures above 2700°C.

12. Gas jet

The gas jet is heated to maintain laminar flow. A heater temperature of approximately 500°C is obtained if the variac control is set to 80% with a nitrogen flow rate of 3 liters/minute.

The aerodynamic levitation force of the gas jet results from a decrease in the gas momentum as it passes over the levitated sample. This effect is expressed by the equation:

$$Mg = \Delta \dot{m}u = F\dot{m}u \quad (12-1)$$

M is the sample mass in grams. Gravity is $g = 980 \text{ cm/s}^2$, $\dot{m}u$, \dot{m} , and u are the momentum flow rate, mass flow rate, and exit velocity of gas from the mullite tube, with \dot{m} and u measured in g/s and cm/s, respectively. The quantity F is the fraction by which jet momentum flow rate decreases due to interaction with the sample. In experiments with the gas jet assembly, levitation of a 2.5 mm diameter sapphire sphere in nitrogen gas was obtained at a heater temperature of 536K and flow rate of 2880 cm³(STP)/min = 0.06003 g/s. Using the heater temperature to calculate an upper limit on jet exit velocity gives $u < 2150 \text{ cm/s}$ and $F > 0.246$, with sapphire density taken equal to 3.95 g/cm³.

Purely aerodynamic levitation in a gas jet is stabilized by a combination of lift, drag, and gravity forces. The effect is illustrated in Figure 36 for levitation in an inclined gas jet. The figure illustrates that the three forces can result in an equilibrium levitation position below the centerline of the gas jet, in which rotation is induced by unequal flow rates over opposite sides of the sphere.

In the experiment with a 2.5 mm sapphire sphere, levitation failed when the heater temperature decreased to 515K, i.e., by 4% of its initial value of 536K, while holding the gas flow rate constant. A similar percentage decrease in the gas flow rate, with the heater temperature constant, also led to failure of gas jet levitation. Aero-acoustic levitation is less sensitive to the flow conditions, because the acoustic forces maintain stability over larger variation in the aerodynamic force. This is an essential feature in the use of the aero-acoustic method while melting levitated solids at high temperature, because melting changes the sample shape to produce changes in the aerodynamic levitation force. Once a molten sample has been formed, the gas jet flow rate may be adjusted to precisely balance gravity, and the acoustic forces that stabilize levitation may then be reduced. The MKS flow controller allows precise adjustment of the gas flow rate so that the aerodynamic force may be adjusted to precisely balance the force of gravity.

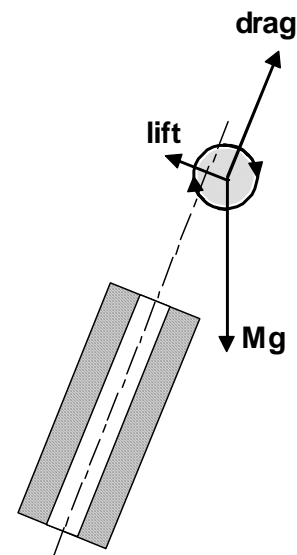


Figure 36 Levitation in an inclined gas jet.

Stable levitation requires a smooth decrease in aerodynamic force with distance in the gas jet, i.e., a slowly diverging laminar jet flow. This condition requires that the Reynolds' number, Re , characterizing gas flow in the mullite tube be significantly less than 2,000, above which turbulent flow will occur in the flow tube. Laminar flow is maintained at a greater distance in the gas jet for smaller values of Re . The value of Re is given by the equation:

$$Re = \frac{\rho u d}{\mu} = \frac{4\dot{m}}{\pi d \mu} \quad (12-2)$$

Here, ρ , μ , and d are the gas density (g/cm^3), gas viscosity (poise, $\text{g cm}^{-1}\text{s}^{-1}$) and jet diameter (cm). The viscosity of a gas increases with temperature so that heating the gas maintains laminar flow in the gas jet for a few cm from the flow tube exit.

Figures 37 and 38 illustrate the effects of heating the gas jet on the density of materials that may be levitated and on the values of Re obtained. In Figure 37, the density is plotted vs gas flow rate, for gas temperatures of 536K and 800K. Smaller flow rates are required with a higher temperature gas, because at constant flow rate, gas velocity and momentum flow rate increase with temperature. The black Density of 2.5 mm specimens levitated in N_2 . Reynolds number, Re , of a nitrogen jet at 300, 536, and 800K. circle plotted on the curve for 536K represents the 2.5 mm sapphire levitation experiment discussed earlier.

The curves in Figure 38 were calculated assuming a constant value for the quantity "F" in equation (12.1), i.e., that the fraction of the momentum flow rate in the jet that is converted to a levitation force does not vary with the flow conditions. In fact, one would expect the levitation efficiency to vary slightly with the value of Re due to variation in the spreading of the jet with distance from the flow tube and with the sample diameter.

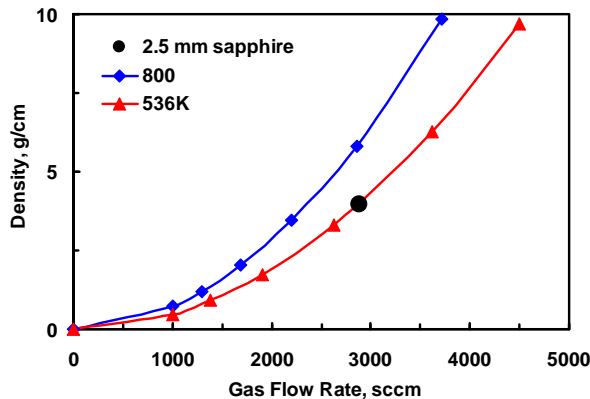


Figure 37 Density of 2.5 mm specimens levitated in nitrogen.

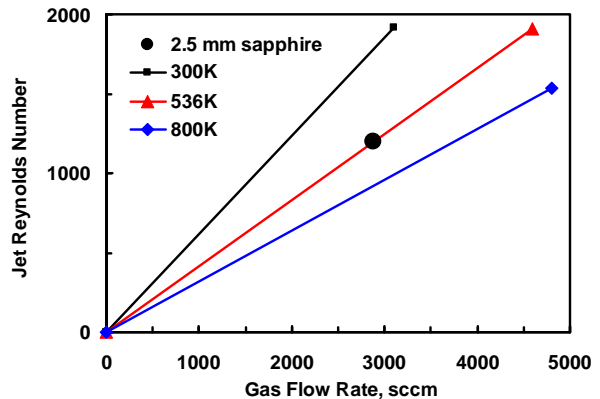
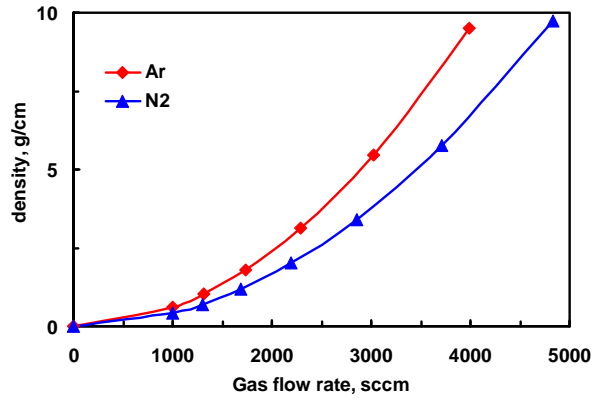


Figure 38 Reynolds number, Re , of a nitrogen jet at 300, 536, and 800K.

The 2.5 mm sapphire levitation condition is marked in the figures. $Re \approx 1200$ is sufficient to maintain levitation (in this case at a distance ca. 2.5 cm above the mullite flow tube). Figure 39 compares the density of materials levitated in nitrogen and argon gas jets. A heater temperature of 800K and 3 mm diameter sample were assumed in calculating these results. It was also assumed that 25% of the momentum flow rate is converted to levitation force, as previously measured for a 2.5 mm sample. Equality in this factor for argon and nitrogen flows is a good assumption because the Reynolds numbers for argon and nitrogen jets are nearly equal for equal volumetric flow rates. Since nitrogen is lighter than argon, an argon jet can support denser materials at equal volumetric flow rates.



F
Figure 39 Estimated density of 3 mm specimens levitated in argon and nitrogen jets.

13. Position Sensing Operations

The analog detector electronics produce two voltages, V_Y and V_{Ref} . V_Y is proportional to the total intensity and to the position of the sample shadow on the detector. V_{Ref} is proportional to the total intensity. The digital detector electronics obtains the AC component of these signals then calculates the ratio, V_Y/V_{Ref} to obtain a result that is independent of total intensity. The value, Y , is calculated as the position signal proportional to distance along the acoustic axis as:

$$Y = 5 \frac{V_Y}{V_{Ref}} \quad (8.1)$$

The sensitivity of the position-sensing signal to sample position was calibrated by moving an acoustically levitated sample through 400° of phase change for transducer A on each axis. The sample distance change equals half a wavelength for 360° of phase change for the transducer. The acoustic wavelength, λ for given sound speed U_S and frequency, F , is:

$$\lambda = \frac{U_s}{F} = \frac{1}{F} \sqrt{\frac{\gamma RT}{M}} \quad (8.2)$$

Here $\gamma = CP/CV$ is the constant pressure to constant volume heat capacity ratio, 1.40 for air. We take $T = 298K$, $M = 29$ amu, and $R = 8.31 \times 10^7$ for these units to obtain $U_S = 34,576$ cm/s and $\lambda = 1.571$ cm at the acoustic frequency, $F = 22,000$ Hz. Figure 40 plots the sensor output vs sample position. The equation given in the figure fits the region $\pm 40^\circ$, or ± 0.87 mm about the center, the approximate upper limits on position fluctuations of levitated samples.

The slope of such plots is used to calculate relative position-sensing sensitivities for the three acoustic axes that are entered in the sensor screen of the GUI.

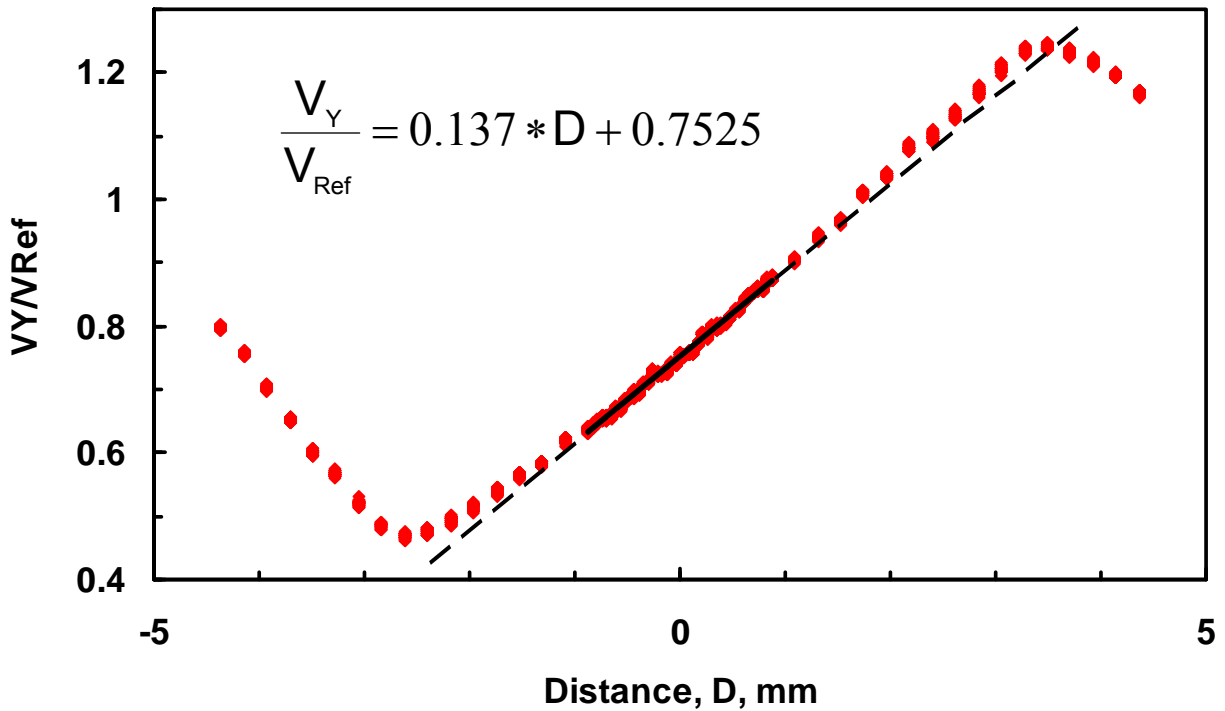


Figure 40 Sensor output vs position of a levitated sample.

13.1 Feedback Control for Damping Oscillation of Levitated Samples

Feedback control of the acoustic phases is used to maintain stable levitation at the desired position. This position is at the intersection point of the three acoustic axes, on the gas jet axis, and centered in the beams of the sample heating lasers. It is marked on the video camera monitors.

1. An operator controls the gas flow rate to support the levitated sample at the desired position.

Careful adjustment of the gas flow rate allows levitation with relatively small values of the SPL. SPL is typically increased when a sample is initially levitated, or heated through the melting point.

2. An operator controls the acoustic phase differences for each set of opposed acoustic transducers.

The phase differences are initially set at 180° to produce an acoustic node exactly half-way between the transducers in a uniform temperature gas. Slight adjustments in the phase

differences are made by the operator to compensate for asymmetry in the sound speed that develops with the heated gas jet and laser-heated sample.

Heating of the sample increases the gas temperature in the sample wake so that the average sound speed will be slightly larger above than below the sample. This means that the phase difference, ϕ , between the upper transducer B and the lower transducer A should be reduced to a value less than 180° to maintain levitation half-way between the two transducers.

3. The sensing system electronics determine the velocity with which a levitated sample oscillates in position. It sends instructions to the acoustic controller that change the acoustic phases in a manner that dampens the sample oscillations.

The sensor outputs are acquired at a rate of 40 KHz as the difference between the on and off intensities of the 808 nm diode lasers. Each set of 160 consecutive measurements is analyzed to obtain sample velocity values, u , at a rate of 250 Hz. Sample velocity is measured as the difference between the sums of the second and first 80 V_Y position measurements in each set, normalized by corresponding sums of V_{Ref} measurements.

The operator specifies a gain value, K_D applied to the velocity calculation that yields a number of degrees, $\Delta\phi$, that the transducer phase will change. Each velocity measurement results in a change of phase for transducers A and B from the preset values (0° and 180° as at start-up, or as adjusted from these values by the operator for temperature and spin). The phase change for transducers A and B are in opposite directions, limited to $\pm 10^\circ$, to produce a total phase change for the pair that is twice the calculated value. The change in position, Δx , of the acoustic node is given by:

$$\Delta x = \lambda \frac{\Delta\phi}{360} \quad (13.1)$$

The value of Δx depends on sample temperature due to the increase in acoustic wavelength with temperature. Therefore the gain value, K_D may be decreased by the operator as the sample temperature increases to obtain optimum control of sample oscillations. For example, in argon gas, at 300 or 3000°K and 22.2 KHz, a $\pm 10^\circ$ phase change yields $\Delta x = \pm 0.4$ mm and ± 1.3 mm, respectively.

The simple algorithm used to calculate velocity is designed to minimize the time delay between sensor data acquisition and the acoustic phase changes that dampen sample oscillation. The measured delay is less than 8 ms of which 2 ms is inherent in the velocity calculation. The 250 Hz velocity measurement rate is chosen as a sufficient multiple of the 9 Hz or less oscillation frequency of levitated samples, as estimated in section 11.2.

The graphical display on the sensor screen is sensitive to both the position and to the orientation of levitated samples. Therefore, rather high frequency variations in the sensor output are observed when samples spin.

